CHAPTER 1

INTRODUCTION AND LITERATURE REVIEW

As the world becomes more and more industrialized in order to enable the ever-growing population live life in a more comfortable manner, the demand for electricity is witnessing a steep rise. At the same time, the availability of land is making the right-of-way a serious concern, such that it is becoming difficult to establish bigger transmission lines. The decreasing fuel supply has put the onus on the engineers to find ways in order to harness the existing capacity in a better way.

Series capacitive compensation is the most commonly used method of increasing the power transmitted, as it helps by reducing the inductive reactance of the line in contention [1]. As it is not complex and easiest means for transmission line power capability enhancement, it has been used extensively for the same. But it is known to cause an associated problem with the possibility of subsynchronous resonance (SSR) [2]. This phenomenon can be quite dangerous and can potentially lead to permanent damage of the shaft of the turbine-generator used, an occurrence that was first noted in Mojave, USA in 1980 [3] The complex mechanical system involved in power generation gives rise to many possible modes of oscillation, and thus it is critical that such a situation is avoided for the healthy operation of the power system.

IEEE has established benchmark models for the study of SSR [4-5], and over the years, a lot of work has been done and many methods have been devised in order to mitigate the SSR condition. Early strategies suggested the use of filters and other static devices [6], but they are seen to be effective only for particular cases and values of the system [7]. Other methods include dissipating the energy during resonance in resistor banks and phase shifters [8]. The use of Power system stabilizers and their tuning has been studied [9-10] and shown to have a limited positive effect [11]. Stored magnetic energy usage has been published in [12], while utilizing an induction machine damping unit (IMDU) was devised in [13-14].

Post this, with the evolution of FACTS technologies by EPRI [15], a new dimension to power enhancement was witnessed. FACTS controllers are power electronic based devices which can influence transmission system voltage, currents, impedances and/or phase angle in a fast and often continuous manner. Apart from increasing the amount of power transfer, the devices can help in improving the stability of the system [16-18]. Thus, when today's large scale systems need the FACTS push in order to satisfy the power needs, it is only reasonable that solutions to problems like SSR are found in the use of these FACTS devices itself.

FACTS devices are of two types – thyristor based and voltage sourced converter based [19]. While TCR, TCSC, etc are of the former type, the latter include devices such as SSSC, STATCOM and UPFC. The first probable method of a FACTS device used to mitigate SSR was the use of NGH scheme [20]. A shunt scheme involved the use of Static VAR compensators, both by itself and in conjunction with PSS [21-23], and the use of STATCOM, another advanced shunt device, has also been studied [24]. But shunt devices are not widely preferred for power enhancement due to the complexities of their placement in the system. SSSC has also been studied for its use in the SSR mitigation [25]. FACTS devices have also been employed in wind farms to solve the SSR problem [26]

The thyristor controlled series capacitor has been investigated for its usefulness in this regard[27-28], and was found to be a most versatile device in this context, as it involves the modulation of the inherent series capacitance in the line through various control schemes [29-30]. Moreover, series devices have been reported to be more effective than shunt ones in controlling SSR. Studies have shown that TCSC can be useful for this [31-35], and there are several real-time installations that incorporate the mitigation of SSR in their design principle [36-39].

This work analyzes the occurrence of SSR in the IEEE first benchmark model SMIB system in SIMULINK environment, and investigates its mitigation using a PSS and a TCSC. The results of the different feedback signals and appropriate controller configurations are presented to provide a comparative study of the analysis carried out.

CHAPTER 2

SSR AND COMMONLY USED COUNTERMEASURES

The electrical power system comprises electricity generating stations, transmission lines and distribution systems apart from various other controlling equipment for their own working and also to co-ordinate all of the above. The generating stations comprising turbines and generators convert the available mechanical energy, present in the form of water pressure or steam pressure into corresponding electrical energy. This generated electrical energy is then transmitted to the distribution stations through the transmission lines and network. Thus, the transmission lines form power transmission links between the load centres and the generating stations, which are commonly situated large distances apart due to various technical and economical considerations.

2.1 Role of Transmission lines

The role of transmission lines is extremely critical in the effective functioning of a power system. The transmission line plays an important role in transmitting electrical energy from the generating stations to the load centers. In other words they may be viewed as the roads of the power system that helps the subject (power/electricity) reach the destination (load) from the source (generating station). The transmission network is by far the most expensive part of the transmission network. It is essential to have a well developed, high capacity transmission system to make it economic and feasible to transmit large blocks of electrical energy over long distances. It would be definitely better, if the same amount of electrical energy is transmitted over a transmission line having lesser installation cost or the power transmission capability of an existing transmission line is increased.

Any transmission line is made up of material that has both resistive and reactive characteristics. The reactance can be both capacitive and inductive, while the resistance is a function of the material by which the line is made. The formula governing the resistance is given by,

$$R = \frac{\rho l}{a} \qquad (2.1)$$

Where,

ρ = Resistivity of the line material

L = length of the line

A = area of cross section of the line

The inductance of the line is due to the existence of the magnetic lines of force around the conductors, while shunt capacitance (or conductance), which is quite negligible, is due to the relation of the line power flow with respect to the ground. Thus, the inductive reactance plays the dominant role in the power transmission line, leading to an effective decrease in the amount of power transferred as and when the inductance of the line increases.

The power transfer equation of a power system can be given as [1]

$$P = \frac{E\,V}{X} \sin\delta \qquad (2.2)$$

Where,

E – Voltage at generating end (Volts)

V – Voltage at receiving end (Volts)

X – Reactance of the line (ohms)

δ - Angular difference between E and V or the load angle (degrees)

From the above equation, it is inferred that the net power transfer can be increased by:

1. Increasing E and V i.e sending and receiving end voltages, or
2. Increasing δ i.e. the load angle, or
3. Decreasing X i.e. net reactance of the transmission line

Though all the above are theoretically possible and to some extent practically feasible, there are limitations associated with them. If the voltage levels are increased to an extremely high value, the cost of the insulator goes up by an exorbitant amount. Also, it is then imperative to construct more robust power transmission towers. By considering the option of the load angle, we see that

it can be increased only upto a certain level, as beyond that, there is a risk of the system going into instability.

2.2 System compensation using series capacitors

From the above conclusions, it can be understood that the only practically feasible solution over a broad range is the decrease in the effective reactance. As the usual line reactance is inductive, which is conventionally considered as positive, we can decrease the reactance by including a series capacitive reactance, which can be treated as negative.

$$X_{eff} = X_{line} + (-X_c) \quad (2.3)$$

When series compensating capacitors are used to aid the power transmission and increase its levels, a particular phenomenon of variance in the transient torque frequency occurs. The transient torque frequency, following a disturbance, can be seen to vary from 0 to 120 Hz i.e. from the subsynchronous frequency range of 0 – 60 Hz for the positive sequence components, to 60 - 120 Hz called supersynchronous torque. This broad spectrum of frequency indicates that under certain system conditions it may be possible to directly excite the natural frequencies of the mechanical systems.

2.3 Mechanical components in the power system

The rotor of a turbo-generator is a very complex mechanical system. The generator rotor is connected to the last turbine of a group of turbines and the exciter is connected to the rotor at the end. The various sections are coupled together with the help of interconnecting shafts. The rotor of the turbo-generator may itself be over a 100 feet in length and may weigh several hundred tons. With a number of smaller components forming a part of the entire system as a whole, the system possesses several modes of torsional oscillations that can be excited due to various reasons.

2.4 Possibilities of Shaft Damage

When a massive turbo-generator unit as discussed above is connected to a power system, system switching events such as fault occurrence, fault clearance, incorrect synchronizing and reclosing and live switching which generally occurs independent of subsynchronous resonance conditions will have the effect on turbo-generator shafts. Events such as high-speed reclosing consequently decay the fatigue life of the shafts.

Apart from this scenario, it was noticed that sustained oscillation below the fundamental system frequency can be caused by series capacitive compensation. This phenomenon, called Subsynchronous resonance, though first reported in the late 1930s [2], came into prominence only in the 1970s, after two specific incidents of turbo-generator shaft failure occurred at Mojave Generating station in USA [3]. Investigations showed that the interactions between a series capacitor compensated line, oscillating at the natural or subharmonic resonant frequency, and the mechanical system connected to the line set in torsional mechanical oscillation can result in negative damping, with the electrical and mechanical oscillations increasing steadily with time.

2.5 Subsynchronous Resonance (SSR)

Resonance in general is defined as the relatively large selective response of an object or system that vibrates in step (in phase) with an externally applied force. Resonance for electrical systems is defined as the enhancement of the response of a physical system to a periodic excitation when the excitation frequency is equal to a natural frequency of the system. Resonance, therefore, implies a periodic phenomena such as vibration, and two oscillators, one driven at or near its resonant frequency and the other driving as an externally applied force.

The IEEE definition of subsynchronous oscillation is as follows:

“Subsynchronous oscillation is an electric power system condition where the electric network exchanges significant energy with a turbine-generator at one or more of the natural frequencies

of the combined system below the synchronous frequency of the system following a disturbance from equilibrium"

Electrical power generation involves interaction between the electrical and mechanical energies coupled through the generator. It follows that any change in the electric power system results in a corresponding reaction/response from the mechanical system and vice versa. Slow-changing load translates to a slow-changing mechanical torque on the rotor shaft, which in turn, is matched by a slow-changing rotor angle to new steady-state angle between the rotor and the stator along with adjustment in the mechanical power input to the rotor through the turbines. Major disturbances such as faults and fault clearing result in large transient torques on the mechanical system.

A typical rotor of a large turbine-generator consists of several rotating masses. The rotor masses and coupling shafts form a spring-mass system which has intrinsic modes of torsional natural frequencies which are mostly below the synchronous frequency. There are many modes of torsional oscillations for a multi-mass-spring system, in addition to a zero mode by which the entire mass-spring system oscillates as a rigid body.

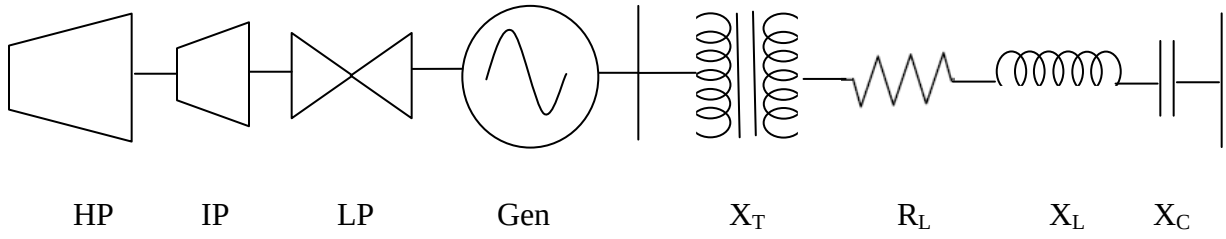

Fig 2.1 Series compensated single machine infinite bus system.

A single machine infinite bus system with the series capacitor compensated transmission line shown in Figure 2.1 will have a resonance frequency f_e given by [11]

$$f_e = f_0\sqrt{\frac{X_C}{X''+X_L+X_T}} = f_0\sqrt{\frac{X_C}{X_{tot}}} \qquad (2.4)$$

Where,

f_0 is system nominal frequency (Hz)

X'' is sub-transient reactance of the generator (pu)

X_T is transformer leakage reactance (pu)

X_L is transmission line inductive reactance (pu)

X_C is the capacitive reactance (pu)

It is often possible that the electrical resonant frequency is close to one of the compliments of torsional oscillation frequency (i.e.) f_0 - f_m. In such a situation, the torsional mode of oscillation gets excited, and sub-synchronous oscillations can originate to lead to disastrous consequences. Also, for each of the modes, there exists a separate resonant frequency, leading to possibilities of multiple resonances depending on the level of compensation used.

Currents of resonant frequency (f_e) in the electrical system give rise to rotor current of frequency f_r as indicated in the equation.

$$f_r = f_0 \pm f_e \qquad (2.5)$$

The armature currents induce an RMF in the armature, and frequency of rotor body currents induced by this field is governed by the relative velocity between the armature field and the rotor. Positive sequence components of stator current produce rotor current at sub synchronous frequency $f_r = f_0 - f_e$. Negative sequence components of the stator current produce rotor current at supersynchronous frequency $f_r = f_0 + f_e$. The sub-synchronous electrical frequency and subsynchronous torque frequency (i.e.) $f_0 - f_e$, are said to be complimentary because they add to unity on the base of the fundamental frequency f_0.

2.6 Types of SSR

SSR can be induced in the system either by self-excitation or by external means (faults). The subsynchronous frequency current entering the generator terminals produces subsynchronous frequency terminal voltage components. These voltage components may sustain the currents to produce self excitation. The self excitation can be classified into Induction generator effect and Torsional interaction, whereas the third type, Torque amplification, is only due to an external disturbance [11]. All three are briefly described below.

2.6.1 Induction generator effect

As the rotating MMF produced by the subsynchronous frequency armature current moves as a speed slower than the speed of the rotor, the resistance of the rotor viewed from the armature terminals is seen as negative, and thus the slip of the machine viewed as an IG is negative. When this negative resistance exceeds the sum of the armature and network resistance at a resonant frequency, there will be self excitation.

2.6.2 Torsional interaction

Generator rotor oscillations at a torsional mode frequency, f_n, induce armature voltage component of subsynchronous and super-synchronous frequency (f_e). The armature voltage frequency components are related to the torsional made frequency by the equation,

$$f_{en} = f_0 \pm f_n \qquad (2.6)$$

When f_{en} is close to f_{er}, the subsynchronous frequency voltage is phased to sustain the subsynchornous torque. If the component of sub-synchronous torque in phase with rotor velocity deviation equals or exceeds the inherent mechanical damping torque of the rotating system, the system will become self excited. This interaction between the electrical and mechanical system can lead to SSR.

2.6.3 Shaft Torque Amplification

System disturbances resulting from switching in the network tend to excite oscillatory torques on the generator rotor. The transient torque might have many components, ranging from subsynchornous to even multiple of the fundamental frequency. Thus, torques may be induced in the shafts following a system disturbance which are much larger than those developed as a result of three phase fault in an uncompensated system. This is due to the resonance effect and the fact that the torsional mode damping in a turbine generator rotor system has been observed to be extremely low. This effect is referred to as shaft torque amplification.

2.7 How Torsional fatigue can lead to shaft damage

Fatigue damage is the process of increasingly localized permanent structural change occurring in the shaft material subject to conditions which produce fluctuating stresses and strains at some points and which may culminate in cracks of complete fracture after a sufficient number of fluctuations. In some systems where the total damage can result in huge secondary problems, even the initiation of a crack is termed as potentially dangerous. Fatigue is not a one-time occurrence but a cumulative process. It is not until all the fatigue life is used up that an observable defect such as a crack will be obtained. Hence, for example, if a shaft system is inspected and no cracks are identified following a severe torsional duty, as the majority of the shaft fatigue life may have been consumed. A few relatively minor disturbances in the future may then initiate a crack and lead to a gross failure.

2.8 Traditional methods to overcome SSR

Use of shunt compensators do not result in electrical resonant frequencies below the synchronous frequency, but rather in supersynchronous frequencies, which can even aid the damping of the oscillations. But shunt compensation cannot be an effective replacement of series compensation, as the latter is economical and the placement of series capacitors in the line does not adversely affect the working of the overall system.

In order to avoid the system oscillation at the subsynchronous frequencies, another solution that was considered was that of designing machines such that the lowest torsional mode frequency is greater than the synchronous frequency. But such a design is not feasible, and changes in the system with upgrades and additional equipment will anyway make it redundant.

Another documented method is that of using a highly nonlinear metal oxide resistor in parallel with the capacitor [11]. During normal operation, very less current flows through the resistor, while during fault, it provides a parallel path and the voltage across the capacitor reaches a saturation level.

Static blocking filters can be used in series with the generator step up transformer winding on the neutral end of the transformer high voltage winding [6]. It is usually a three-phase filter made up of separate filters connected in series. Each section of the filter is a high Q, parallel resonant circuit tuned such that it blocks the current corresponding to the torsional mode. However, the tuning of the filter is affected by changes in the system frequency and temperature sensitivity of the filter capacitor. This along with the problem of huge space requirement and increased insulation level of the generator transformer make the static blocking filter a less preferred option.

Bypass damping filter is most suitable in countering the induction generator effect as it is capable of introducing significant positive resistance in the circuit for subsynchronous oscillation frequencies upto 90% of the system frequency. But the filter is most effective only at lower frequencies, and the effect is negligible at higher frequencies [11]

Other methods devised include usage static phase shifters [8] and magnetic stored energy [12]. An Induction Machine Damping Unit (IMDU) has also been developed in order to mitigate the SSR phenomenon [13-14].

Apart from the above, two of the more prominent methods in eliminating SSR are discussed briefly in the following pages.

2.8.1 NGH Damping scheme

This scheme was conceptualized by N.G.Hingorani and first employed at Southern California Edison's Lugo substation in USA in 1984 [20]. It is seen that if a sinusoidal voltage of fundamental frequency is combined with a DC voltage, some half cycles are longer than the nominal period, and this is observed to be true for any combination of a base signal of fundamental frequency with DC and subsynchronous frequencies. Thus the NGH scheme involves the dissipation of capacitor charges whenever the measured half cycle period exceeds the nominal time period. For this, a resistor is inserted across the capacitor through thyristor switches, and the thyristor ceases to conduct whenever the capacitor voltage reaches zero. Though the scheme is known to be advantageous and less cumbersome as it does not require any

feedback signals, some undamping can result for certain torsional modes that are off-tune (not due to the electrical resonance)

2.8.2 Power system stabilizers (PSS)

The dynamic stability of a system can be improved by providing suitably tuned power system stabilizers on selected generators to provide damping to critical oscillatory modes. The PSS will introduce a component of electrical torque in phase with generator rotor speed deviations resulting in damping of low frequency power oscillations in which the generators are participating. The input to stabilizer signal may be one of the locally available signal such as changes in rotor speed, rotor frequency, accelerating power or any other suitable signal.

It has been seen that PSS can be used to damp out system oscillations [9-10]. When it becomes apparent that the action of some voltage regulators could result in negative damping of the electromechanical oscillations below the full power transfer capability, PSS were introduced as a means to enhance damping through the modulation of the generator excitation so as to extend the power transfer limit. In power system applications, the oscillation frequency may be as low as 0.1 Hz between 2 areas, to perhaps 5 Hz in smaller units oscillating in local mode.

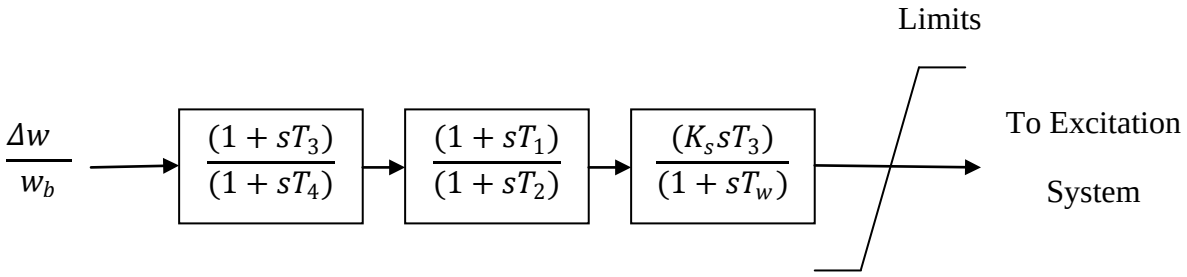

Fig 2.2 PSS configuration

This stabilizing signal is compensated for phase and gain to result in adequate component of electrical torque that results in damping of rotor oscillations and thereby enhance power transmission and generation capabilities. The parameters of the PSS used in the system have been studied by various methods, but it was observed that it is not a very effective means of oscillation mitigation, especially in large multimachine systems [11]

Though most modern generator systems come equipped with a PSS, it has been observed that it alone is not sufficient to damp out the oscillations, and is some cases may even introduce some components that aid them. Thus, FACTS controllers, a new concept that enhances power transmission capability and can provide transient and dynamic stability, are gaining momentum in usage in the modern power systems, and are discussed in the following chapter.

CHAPTER 3

FACTS CONTROLLERS

Flexible AC Transmission systems (FACTS) are a modern power electronic group of devices that aim in helping alleviate the growing power needs. The FACTS technology was initiated by the EPRI in the 1980's to improve controllability of power over existing transmission corridors [15], and they play a principal role in enhancing the capability of the AC systems. Those FACTS devices that have an integrated control function are known as FACTS Controllers, and they are capable of controlling the interrelated line parameters. They also look after other variables that govern the operation of transmission systems, be it the impedances, voltage, current or the phase angle.

3.1 Classification of FACTS controllers

FACTS controllers can be broadly classified as follows:

- Series controllers
- Shunt controllers
- Combined series-series controllers
- Combined series-shunt controllers

3.1.1 Series controllers

Series controllers are used to inject voltage in series with the line, and can be a variable capacitive or inductive reactance, or a power electronics based variable source of main frequency. In most cases the voltage is in phase quadrature with the current, and thus the power transfer is reactive. Any other phase relationship will lead to real power transfer as well. Examples can be static synchronous series compensator (SSSC) and Thyristor-Controlled Series Capacitor (TCSC).

3.1.2 Shunt controllers

These are similar to the series controllers, with the difference being that they inject current into the system at the point of connection. Examples include the Thyristor switched capacitor (TSC), thyristor controlled reactor (TCR), Static VAR compensator (SVC) and the Static synchronous compensator (STATCOM).

3.1.3 Combined series-series controllers

This can be a combination of separate series controllers, which are controlled in a co-ordinated manner, or it can be a unified controller, where separate series controllers provide independent series reactive compensation for each line, but exchange power between each other as well. An example of this is the Interline Power flow controller (IPFC).

3.1.4 Combined series-shunt controllers

This is similar to the combined series-series controllers, but one or more device is connected in shunt. An example is the Unified power flow controller (UPFC).

Some of the commonly used devices are briefly described in the following pages.

3.2 Thyristor-Switched Capacitor (TSC)

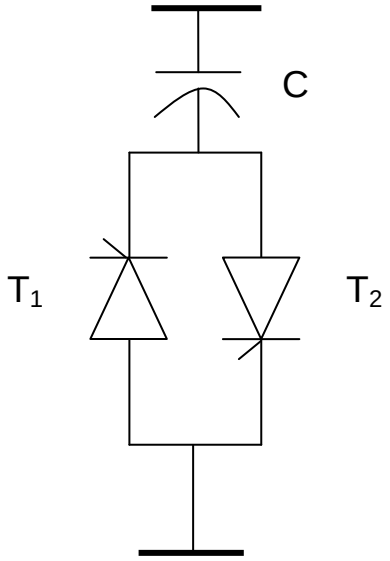

Fig 3.1 Thyristor-Switched Capacitor

A thyristor-switched capacitor (TSC) consists of a fixed capacitor C, a bidirectional thyristor switch SW, and a comparatively small surge-limiting reactor L as shown in Figure 3.1. It can be considered as operating such that it switches a capacitor in or out of the system. Thus, there is only a binary action, and no firing angle control takes place. The TSC can be disconnected at zero current by prior removal of the thyristor-gating signal.

3.3 Thyristor-Controlled Reactor (TCR)

A thyristor-controlled reactor (TCR) consists of a fixed reactor of inductance L and a bidirectional thyristor switch, as shown in Figure 3.2

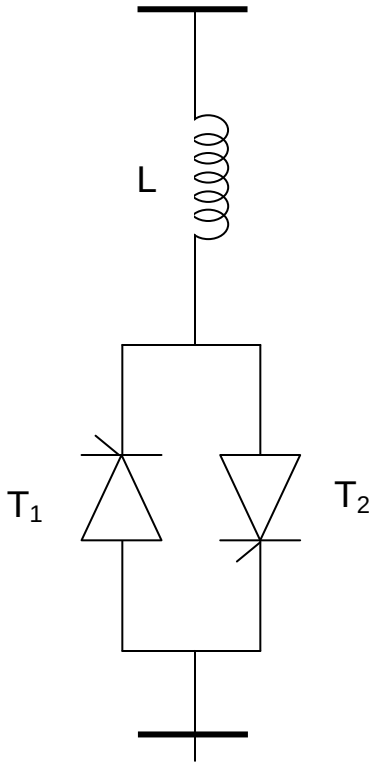

Fig 3.2 Thyristor-Controlled Reactor (TCR)

The current through the reactor can be controlled from zero to a maximum by varying the firing angle of the thyristor. Thus it can be observed that the admittance can be varied by varying the firing angle of conduction of the thyristors.

3.4 Static VAR Compensator (SVC)

If a system employs either TCR or TSC, it would lead to a compensation of only either the inductive component in the former, or only the capacitive component in the latter. But it is often desirable to have both types of compensation, and this is where a static VAR compensator (SVC) is helpful. A SVC consists of TCRs in parallel with one or more TSCs, as can be seen in figure 3.3. The reactive elements are connected to the high voltage system through a step-down transformer. Thus, TCR and TSC can in fact be called subsets of the larger SVC scheme.

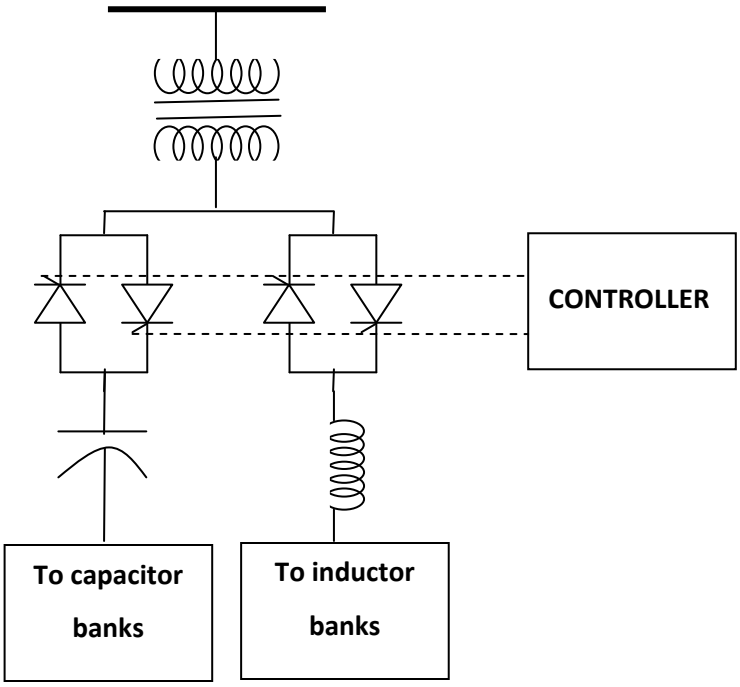

Fig 3.3 Static VAR Compensator (SVC)

3.5 Static Synchronous Compensator (STATCOM)

A Static Synchronous Compensator (STATCOM) can be considered as an advanced form of SVC. It can be a voltage-sourced or a current-sourced converter, and is connected in shunt to the system. Based on whether it has an energy source or not, a STATCOM can be shown to be capable of both real and reactive power transfer.

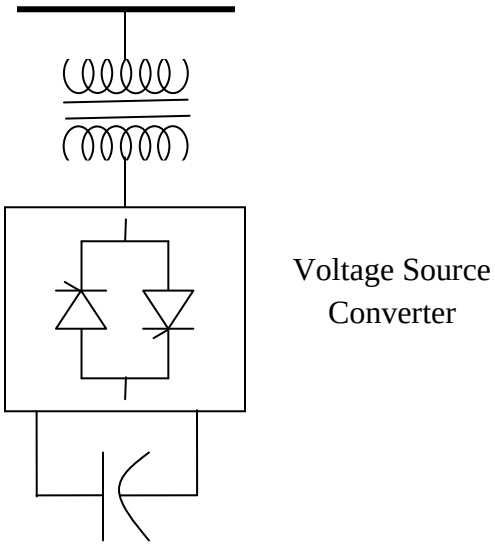

Fig 3.4 Static Synchronous Compensator (STATCOM)

3.6 Static Synchronous Series compensator (SSSC)

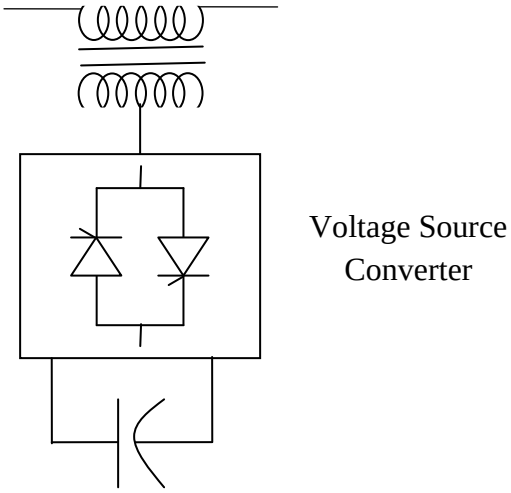

Fig 3.5 Static Synchronous Series Compensator (SSSC)

This device is operated without any external energy source, and the output voltage is in quadrature with the line current, used for the purpose of increasing or decreasing the overall reactive voltage drop across the line, thus controlling the flow of electrical power. The SSSC is one of the most important FACTS devices, and can be both voltage-sourced and current-sourced based.

3.7 Thyristor-Switched Series Capacitor (TSSC)

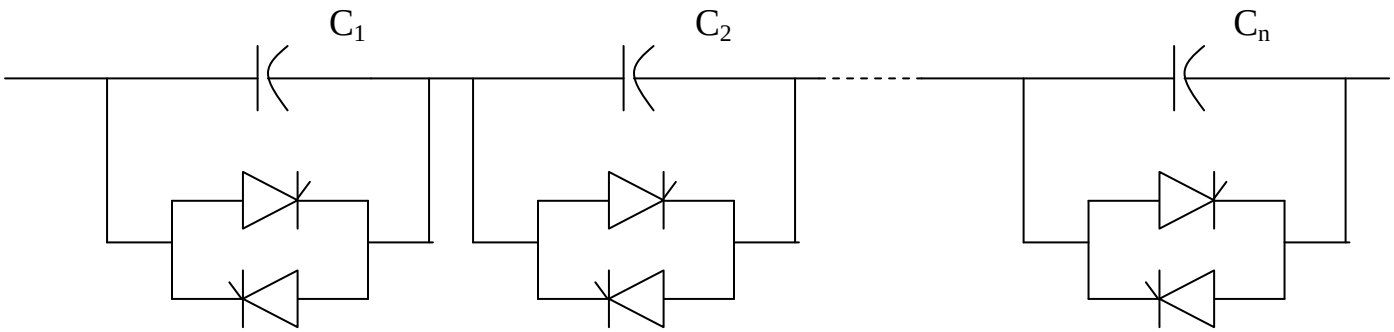

Fig 3.6 Thyristor-Switched Series Capacitor (TSSC)

A thyristor-switched series capacitor (TSSC) consists of a number of capacitors in series, each shunted by a switch composed of two anti-parallel thyristors as shown in fig 3.6. A capacitor is inserted in the transmission line by turning *'off'* the thyristors, and it is bypassed by turning *'on'* the thyristor switch. The equivalent capacitance, for $C_1 = C_2 \ldots = C_1$ is:

$C_{eq} = C/n$ if n Thyristor switches are switched off

$C_{eq} = 0$ if all the Thyristor switches are switched on

3.8 Thyristor-Controlled Series Capacitor (TCSC)

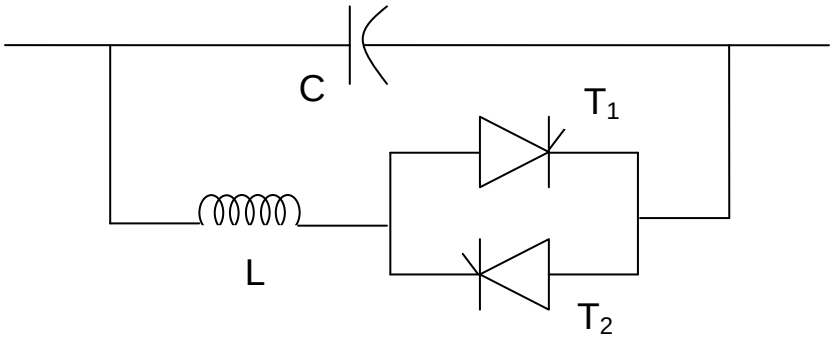

Fig 3.7 Thyristor-Controlled Series Capacitor (TCSC)

The thyristor controlled series capacitor can be viewed as an improvement to the TSC scheme, which provides only a binary control of the capacitor. Though the former is connected in shunt, in the TCSC, which is operated in series with the line, a capacitor in parallel with a TCR model

generates a continuous variable reactance in the line. Thus, this smooth control can be leveraged to provide series compensation of the desired level.

Though various FACTS devices have been seen to provide beneficial results in the field of SSR mitigation, it has been observed that as modern power systems demand the increasing usage of series compensation, the TCSC, with its simple structure and concept of variable reactance, can be one of the most effective in solving SSR problems. The following chapter will provide a detailed analysis of the TCSC operation, characteristics and control structure, leading to an understanding of how it can help in alleviating the SSR phenomenon.

CHAPTER 4

THYRISTOR CONTROLLED SERIES CAPACITOR

4.1 Introduction

The basic thyristor controlled series capacitor scheme was proposed in 1986 by Vithayathil as a means of rapid adjustment of network impedance [19]. The TCSC is composed of a series-compensating capacitor in parallel with a thyristor-controlled reactor. A TCSC is a series-controlled capacitive reactance that can provide continuous control of power on the ac line over a wide range. The scheme is shown in figure 4.1

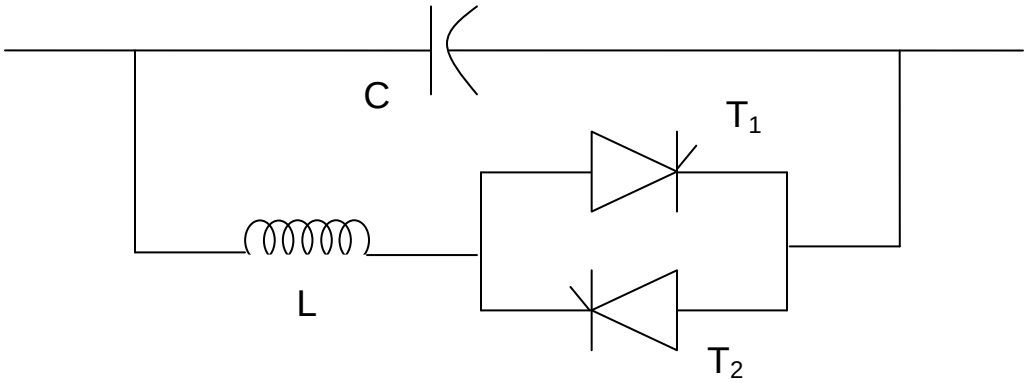

Fig 4.1 TCSC scheme

The principle of variable-series compensation is to increase the voltage across a fixed capacitor (FC) in a series compensated line through appropriate variation of the firing angle, α. Thus the TSSC can be assumed to be a special case of the TCSC, as it operates in a purely on/off manner. The basic operating principle behind the TCSC is that it can provide a continuously variable capacitor by means of partially canceling the effective compensating inductive reactance of the thyristor-controlled reactor.

However, a practical TCSC module also includes protective equipment normally installed with series capacitors. A metal-oxide varistor (MOV), essentially a nonlinear resistor, is connected across the series capacitor to prevent the occurrence of high-capacitor over- voltages. Not only does the MOV limit the voltage across the capacitor, but it allows the capacitor to remain in

circuit even during fault conditions and helps improve the transient stability. Also installed across the capacitor is a circuit breaker, CB, for controlling its insertion in the line. In addition, the CB bypasses the capacitor if severe fault or equipment-malfunction events occur. A current-limiting inductor, L_d, is incorporated in the circuit to restrict both the magnitude and the frequency of the capacitor current during the capacitor-bypass operation. An actual TCSC system usually comprises a cascaded combination of many such TCSC modules, together with a fixed-series capacitor, C_F. This fixed series capacitor is provided primarily to minimize costs.

The World's first TCSC was installed in 1992 in Kayenta substation, Arizona, [36] and it helped improve the transmission capacity by around 30%

4.2 TCSC modes of operation

There are essentially three modes of TCSC operation:

- Bypassed Thyristor Mode
- Blocked Thyristor Mode
- Partially Conducting Thyristor Mode or Vernier mode

4.2.1 Bypassed Thyristor Mode

In the bypassed mode, the thyristors are made to fully conduct with a conduction angle of 180º. Gate pulses are applied as soon as the voltage across the thyristors reaches zero and becomes positive, resulting in a continuous current flow through the thyristor valves.
Thus, in this mode, the TCSC module behaves like a parallel capacitor-inductor combination. However, the net current through the entire module remains inductive, as the susceptance of the reactor is chosen to be always greater than the capacitor.

4.2.2 Blocked Thyristor mode

This mode is also called waiting mode, the firing pulses to the thyristor valves are completely blocked. If the thyristors are in conduction and a blocking mode is suddenly given, the thyristors turn off as soon as the current in them reaches a zero crossing. The TCSC module is thus

effectively modified to a fixed series capacitor, and the net series reactance is nearly purely capacitive.

4.2.3 Partially Conducting Thyristor Mode or Vernier Mode

This mode is of utmost interest in SSR studies, as it allows the TCSC to behave either as a continuously controllable capacitive reactance or, on the other ends, a continuously controllable inductive reactance. This is achieved by varying the thyristor-pair firing angle in the appropriate range. But due to the characteristics of the TCSC, there is no smooth transition between the two modes, as resonant regions exist in between.

This mode can be classified into two types – the capacitive vernier control mode, and the inductive vernier control mode. In the former, the thyristors are fired when the capacitor voltage and capacitor current have opposite polarity. This condition causes a TCR current that has a direction opposite to the capacitor current, resulting in a loop current flow in the TCSC controller.

The working of the parallel LC circuit determines the impedance of the TCSC. The impedance of the TCSC as a function of the delay angle α [19] is illustrated by equation 4.1

$$X_{TCSC}(\alpha) = \frac{X_C X_L(\alpha)}{X_L(\alpha) - X_C} \tag{4.1}$$

Where, the inductive reactance as a function of α is given as,

$$X_L(\alpha) = X_L \frac{\pi}{\pi - 2\alpha - \sin\alpha} \tag{4.2}$$

Where, $X_L \leq X_L(\alpha) \leq \infty$

X_L from equation is ωL and the delay angle α is measured from the crest of the capacitor voltage or the zero crossing of the line current. As the impedance of the controllable reactor is varied from its maximum (infinity) to its minimum (ωL), the minimum capacitive compensation is increased by $X_{TCSCmin} = X_C = \frac{1}{wC}$. Thus, the degree of series capacitive compensation is increased. When $X_C = X_L(\alpha)$, the impedance of the TCSC becomes infinite. Thus, the TCSC

has two operating ranges; one is when $\alpha_{Clim} \leq \alpha \leq \pi/2$, where the TCSC is in capacitive mode. The other range of operation is $0 \leq \alpha \leq \alpha_{Llim}$, where the TCSC is in inductive mode.

4.2 Analysis of TCSC

For consideration of mitigation of SSR study, the analysis of the TCSC operating in Vernier Mode is carried out. The independent variable is the transmission line current, and it is taken as an external current source for simplification. The line current is assumed to be sinusoidal, which is true in the majority of the cases [19]

The current through the fixed capacitor, C, is expressed as,

$$C \frac{dV_C}{dt} = i_S(t) - i_T(t).a \tag{4.3}$$

The term 'a' is employed as a switching variable, and its value is 1 when the thyristor valves are conducting, while it is taken as 0 (so only 1st term exists) when the thyristor valves are blocked. Now, the thyristor valve current, $i_T(t)$ is described as,

$$L \frac{di_T}{dt} = v_C.a \tag{4.4}$$

And the line current, $i_S(t)$ is given by the relation,

$$i_S(t) = I_m \cos wt \tag{4.5}$$

The solution of the above equations lies in the knowledge of the instants of switching. In equidistant firing pulse control, most frequently used because of balanced TCSC operation, the thyristors are switched on twice during each cycle of line currents, say at instants t_1 and t_2,

$$t_1 = -\frac{\beta}{w} \text{ and } t_2 = -\frac{\pi-\beta}{w} \tag{4.6}$$

Here, β is termed as the angle of advance. It can also be expressed as,

$$\beta = \pi - \alpha \; ; 0 < \beta < \beta_{max}$$

The thyristor, modeled as a switch, can be assumed to turn off at the below instances,

$$t_3 = t_1 + \frac{\sigma}{w} \text{ and } t_4 = t_2 + \frac{\sigma}{w} \quad (4.7)$$

Where σ is the conduction angle, and is the same in both the cycles of conduction. Also,

$$\sigma = 2\beta \quad (4.8)$$

By solving the above equations, the steady state thyristor current, i_T is given as,

$$i_T(t) = \frac{k^2}{k^2-2} Imag\ (\cos wt - \frac{\cos\beta}{\cos k\beta} \cos w_r t) \quad (4.9)$$

Where,

$-\beta \leq \text{wt} \leq \beta$

$$w_r = \frac{1}{\sqrt{LC}}$$

$$k = \frac{w_r}{w} = \sqrt{\frac{1}{wL}\frac{1}{wC}} = \sqrt{\frac{X_C}{X_L}}$$

In the above relation of k, X_C is the nominal reactance of the fixed capacitor of the TCSC alone.

Now, the steady state capacitor voltage at the instant wt = -β is expressed by,

$$v_{C1} = \frac{I_m X_C}{k^2-1} (\sin\beta - k\cos\beta\ \tan k\beta) \quad (4.10)$$

At wt = β, $i_T = 0$, and the capacitor voltage is given by,

$$v_C\ (\text{wt} = \beta) = v_{C1} = -v_{C2} \quad (4.11)$$

The capacitor voltage then becomes,

$$v_C(t) = \frac{I_m X_C}{k^2-1} (-\sin wt - k\frac{\cos\beta}{\cos k\beta} \sin w_r t) \quad (4.12)$$

$$v_C(t) = v_{C2} + I_m X_C (\sin wt - \sin\beta) \quad (4.13)$$

Because of the nonsinusoidal nature of the capacitor voltage, the fundamental component, v_{CF} is obtained as,

$$V_{CF} = \frac{4}{\pi} \int_0^{\frac{\pi}{2}} v_C(t) \sin wt \; d(wt) \tag{4.14}$$

The equivalent TCSC reactance is now computed as a ratio of v_{C1}.

The effective impedance of the TCSC works out to be,

$$X_{TCSC} = \frac{V_{CF}}{I_m} = X_C - \frac{{X_C}^2}{X_C - X_L} \frac{2\beta + \sin 2\beta}{\pi} + \frac{4{X_C}^2}{X_C - X_L} \frac{(\cos \beta)^2}{(k^2 - 1)} \frac{(k \tan k\beta - \tan \beta)}{\pi} \tag{4.15}$$

When expressing this relation on pu of X_C, the net reactance is given as,

$$X_{net} = 1 - \frac{X_C}{X_C - X_L} \frac{2\beta + \sin 2\beta}{\pi} + \frac{4X_C}{X_C - X_L} \frac{(\cos \beta)^2}{(k^2 - 1)} \frac{(k \tan k\beta - \tan \beta)}{\pi} \tag{4.16}$$

Writing it in terms of the conduction angle,

$$X_{net} = 1 - \frac{X_C}{X_C - X_L} \frac{\sigma + \sin \sigma}{\pi} + \frac{4X_C}{X_C - X_L} \frac{(\cos \sigma/2)^2}{(k^2 - 1)} \frac{(k \tan k\sigma/2 - \tan \sigma/2)}{\pi} \tag{4.17}$$

As the TCSC is primarily used as a capacitive device, the above derivation assumes a positive sign for the fixed capacitance. While implementing in conventional network studies, this is to be reversed.

The variation of the per unit TCSC reactance (X_{TCSC}/X_C) as a function of the firing angle is given in figure 4.2. It can be seen that a parallel resonance is created between the X_L and X_C at the fundamental frequency, corresponding to the firing angles α_{res}, given by

$$\alpha_{res} = \pi - (2m - 1)\frac{\pi w}{2w_r}$$

Or, in terms of the advance angle,

$$\beta_{res} = (2m - 1)\frac{\pi w}{2w_r}$$

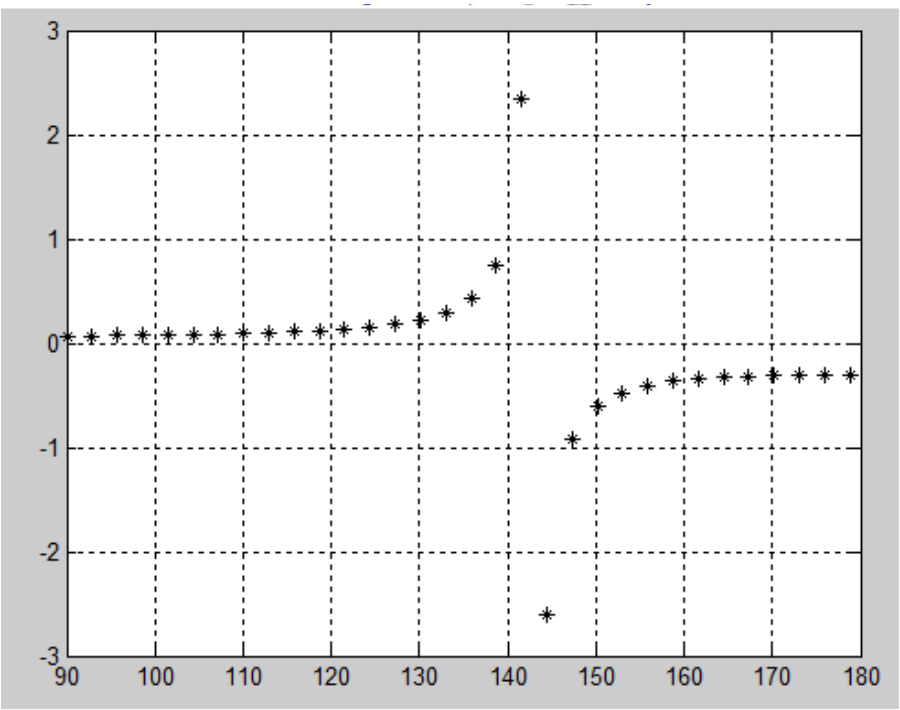

Fig 4.2 TCSC Reactance Vs Firing Angle Characteristics

It is to be noted that different resonances can be inducted into the TCSC characteristics, but this can be avoided by a proper selection of the parameter k. An example to be noted is the TCSC installation at Kayenta [36], where choosing L = 0.0068 H across the 177 μF capacitor results in only one resonant point at 143º, while if L = 0.0043 H, it would lead to resonance at both 101º and 160º, which results in extremely high impedance profile with a substantial drop in the voltage. To avoid this, limits on the firing angle can be implemented, with the most commonly occurring resonant point being 145º. A sample single resonance point characteristics of the TCSC is shown in figure 4.2. It is understood that the Vernier operation helps in the enhancement of the TCSC reactance, whether inductive or capacitive, and does not work in the other way of reactance reduction.

4.3 TCSC Control schemes

To control the TCSC operations, two models are used in practice, as described below.

4.3.1 Variable Reactance model

The variable reactance TCSC model is the simpler of the two, and directly varies the reactance provided by the TCSC using feedback signals from the system under consideration. A sample illustration is shown in figure 4.3

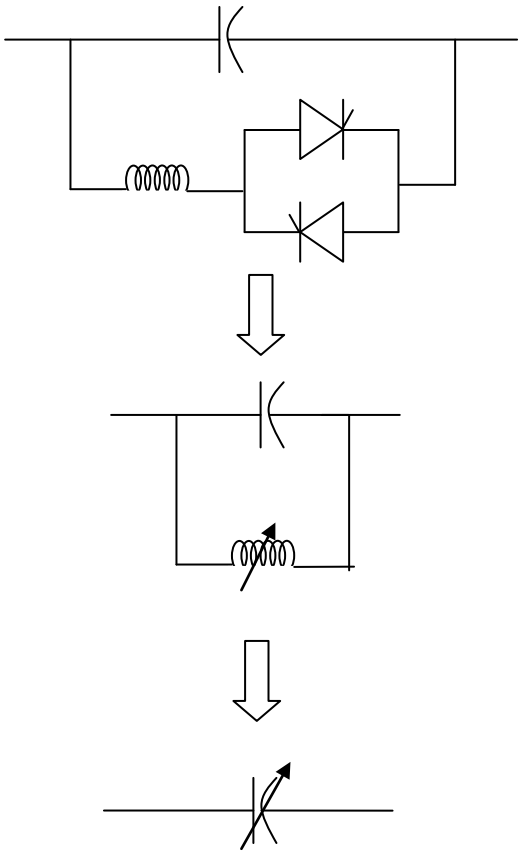

Fig 4.3 TCSC as a variable capacitive reactance

4.3.2 Firing angle control model

This is the more advanced model and it directly the TCSC reactance–firing angle characteristic, given in the form of a nonlinear relation. The reference parameter can be the line current, voltage or the power, and the scheme is modified correspondingly. The basic structure is shown in fig. The line parameter is sensed and compared with the reference value. This error signal is then fed through appropriate gain stages, and then through a linearization block, that helps convert the impedance signal into an equivalent firing angle value. This is then converted into a pulse signal using a firing pulse generator, which is used to fire the thyristors that are part of the TCSC [29-30]

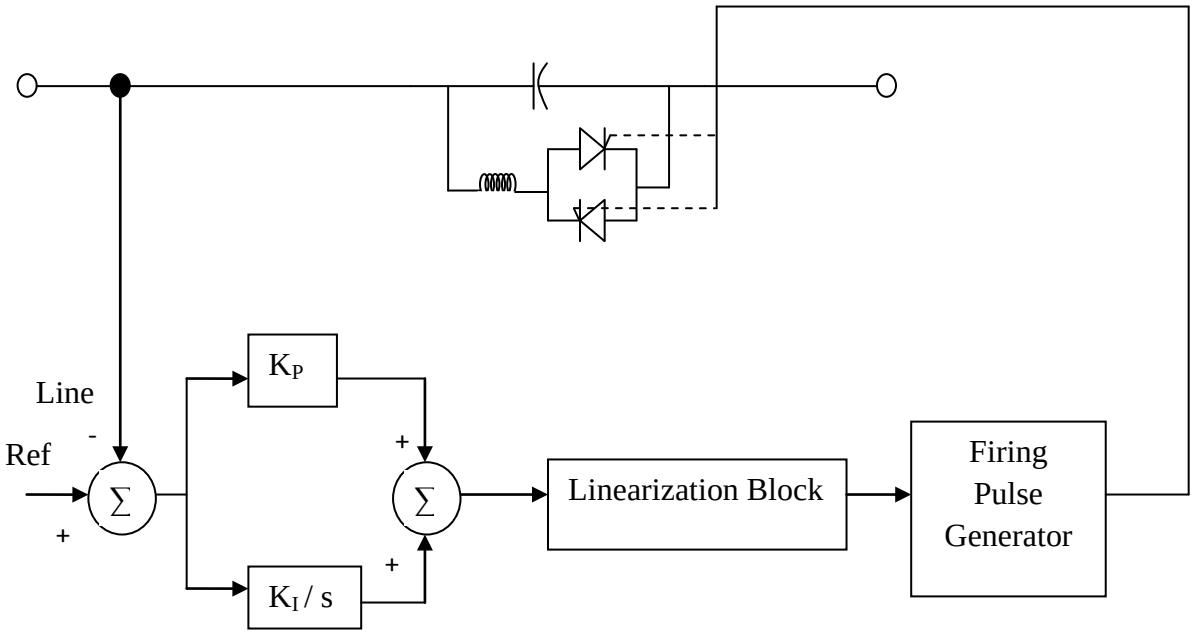

Fig 4.4 TCSC Firing angle control scheme

4.4 Advantages of TCSC:

The usage of TCSC has various definite advantages, such as:

- Rapid and continuous control of transmission line series compensation level
- Damping of power swings from local and inter-area oscillations.
- Voltage support, as the TCSC in conjunction with series capacitors can generate reactive power that increases with line loading, aiding regulation of local network voltages and alleviation of voltage instability.

Over the years, apart from enhancing the power transmission capability, it was noted that the TCSC can prove to be an efficient device to provide damping of electromechanical oscillations, and can thus be a means of series compensation and counter SSR. The benefits with regards to SSR mitigation has been well documented [31-35], and many TCSC installations have been made to this effect[36-39].

In the following chapters, the IEEE first benchmark model will be used to simulate SSR phenomenon. The mitigation of the SSR occurrence will be carried out using a conventional method (PSS), and then a TCSC designed for this specific purpose will be simulated.

CHAPTER 5

SYSTEM MODELLING FOR SSR STUDY

For the analysis of SSR phenomenon and its mitigation, the IEEE 1st benchmark model [4] will be utilized. This consists of an SMIB system with a series capacitor in order to provide enhanced power transfer capability. The system is represented in figure 5.1, and its parameters are given in Appendix 1.

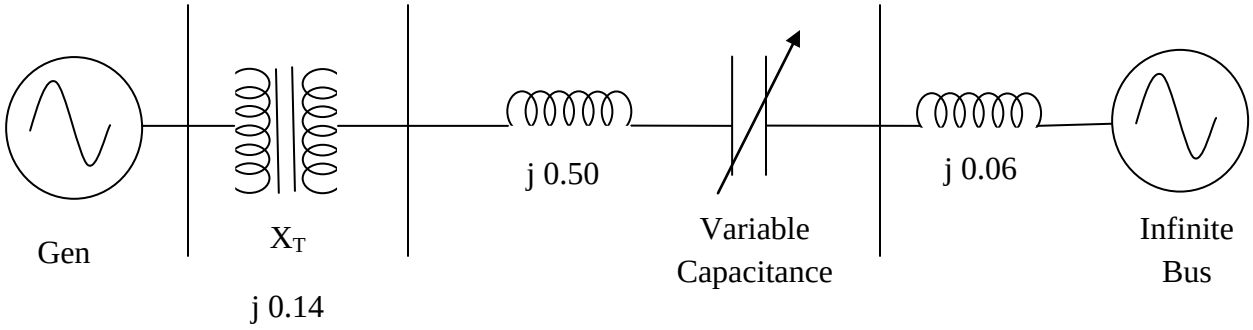

Fig 5.1 IEEE 1st Benchmark model

In order to carry out the simulation, each of the components (i.e.) machine, transmission line and series capacitance are modeled individually in the following pages, and then the final SIMULINK model is realized by combining all of them.

5.1 Mechanical System

5.1.1 Machine modeling

In order to derive the mathematical equations of the machine [40], an understanding of the variation of inductances with the rotor positions will be helpful. Though the MMFs of rotor winding are directed along d and q axes, the resultant MMF will vary. Considering the magnetic effect of only the phase a current, it is seen that the a phase MMF, denoted by Fa, generates flux components,

$$\varphi_d = P_d F_a \sin\theta_r \;\; and \;\; \varphi_q = P_q F_q \sin\theta_q \qquad (5.1)$$

The flux linkage of these resolved flux components is given by,

$$\lambda_{aa} = N_s F_s\left(\frac{P_d+P_q}{2} - \frac{P_d+P_q}{2}\cos 2\theta_r\right) \quad (5.2)$$

Similarly, the flux linkage due to the b-phase component is given by,

$$\lambda_{ab} = N_s F_s\left(-\frac{P_d+P_q}{4} - \frac{P_d-P_q}{2}\cos 2\left(\theta_r - \frac{\pi}{3}\right)\right) \quad (5.3)$$

Thus, the self inductance of the stator a phase winding, if the leakage is neglected, is given as,

$$L_{aa} = L_0 - L_{ms}\cos 2\theta_r \quad (5.4)$$

Similarly, the mutual inductance between a and b phases is given as,

$$L_{aa} = L_{aa} = -\frac{L_0}{2} - L_{ms}\cos 2\left(\theta_r - \frac{\pi}{3}\right) \quad (5.5)$$

The voltage applied to each of the windings in fig 5. Can be balanced using a resistive drop and a differential flux linkage term, which can be represented as below:

$$\begin{bmatrix} v_s \\ v_r \end{bmatrix} = \begin{bmatrix} r_s & 0 \\ 0 & r_r \end{bmatrix}\begin{bmatrix} i_s \\ i_r \end{bmatrix} + \frac{d}{dt}\begin{bmatrix} \Lambda_s \\ \Lambda_r \end{bmatrix} \quad (5.6)$$

In the above relation, the terms of the matrix are in actuality vectors, given below,

$v_s = [v_a \quad v_b \quad v_c]^t$

$v_r = [v_f \quad v_{kd} \quad v_g \quad v_{kq}]^t$

$i_s = [i_a \quad i_b \quad i_c]^t$

$i_r = [i_f \quad i_{kd} \quad i_g \quad i_{kq}]^t$

$r_s = diag[r_a \quad r_b \quad r_c]$

$r_r = diag[r_f \quad r_{kd} \quad r_g \quad r_{kq}]$

$\Lambda_s = [\lambda_a \quad \lambda_b \quad \lambda_c]^t$

$\Lambda_r = [\lambda_f \quad \lambda_{kd} \quad \lambda_g \quad \lambda_{kq}]^t$

When expressing parameters in per phase basis, the notations used are as follows,

r_s – stator winding resistance

r_f – d-axis field winding resistance

r_g – q-axis field winding resistance

r_{kd} – d-axis damper winding resistance

r_{kq} – q-axis damper winding resistance

While transforming the stator quantities to the qd0 reference frame attached to the rotor, it is seen that the resultant voltage equation is found to be time-invariant. The qd0 transformation is applied only to the stator quantities, as the rotor is already along those axes. Let the augmented transformation matrix be given as,

$$C = \begin{bmatrix} T_{qd0}(\theta_r) & \\ & U \end{bmatrix} \tag{5.7}$$

U is a unit matrix, while,

$$T_{qd0}(\theta_r) = \frac{2}{3}\begin{bmatrix} \cos\theta_r & \cos(\theta_r - \frac{2\pi}{3}) & \cos(\theta_r - \frac{2\pi}{3}) \\ \sin\theta_r & \sin(\theta_r - \frac{2\pi}{3}) & \sin(\theta_r - \frac{2\pi}{3}) \\ \frac{1}{2} & \frac{1}{2} & \frac{1}{2} \end{bmatrix} \tag{5.8}$$

Thus, applying the above relation to the stator quantities, the stator voltage equations become,

$$v_{qd0} = T_{qd0} r_s {T_{qd0}}^{-1} i_{qd0} + T_{qd0} \frac{d}{dt} {T_{qd0}}^{-1} \Lambda_{qd0} \tag{5.9}$$

Taking all phase resistances to be equal, the first term reduces to $r_s i_{qd0}$, while the second term can be written as,

$$T_{qd0}[\left(\frac{d}{dt}{T_{qd0}}^{-1}\right)\Lambda_{qd0} + {T_{qd0}}^{-1}\frac{d}{dt}\Lambda_{qd0}] \tag{5.10}$$

Substituting for the transformation matrix, it is seen that the stator voltage equation of now becomes,

$$v_{qd0} = r_s i_{qd0} + w_r \begin{bmatrix} 0 & 1 & 0 \\ -1 & 0 & 0 \\ 0 & 0 & 0 \end{bmatrix} \Lambda_{qd0} + \frac{d}{dt}\Lambda_{qd0} \tag{5.11}$$

Where w_r denotes $\frac{d\theta_r}{dt}$ in electrical radians/sec.

The expression for Electromagnetic torque being developed in the airgap can be derived using the component of input power transferred across it. Let the total input power be given by the relation,

$$P_{in} = v_a i_a + v_b i_b + v_c i_c + v_f i_f + v_g i_g \quad (5.12)$$

Transforming the input power into the rotor's qd0 reference frame, eqn becomes,

$$P_{in} = \frac{3}{2}\left(r_s\left({i_q}^2 + {i_d}^2\right) + i_q \frac{d\lambda_q}{dt} + i_d \frac{d\lambda_d}{dt} + w_r\left(\lambda_d i_q - \lambda_q i_d\right)\right) + 3{i_0}^2 r_0 + 3i_0 \frac{d\lambda_0}{dt} + {i_f}^2 r_f +$$

$$i_f \frac{d\lambda_f}{dt} + {i_g}^2 r_g + i_g \frac{d\lambda_g}{dt} \quad (5.13)$$

When terms that are related to the ohmic losses can be eliminated from the above relation, the relation for electromechanical power is given as,

$$P_{em} = \frac{3}{2} w_r (\lambda_d i_q - \lambda_q i_d) \quad (5.14)$$

Writing the speed in terms of mechanical radians and deriving the relation for the electromechanical torque,

$$P_{em} = \frac{3}{2}\frac{P}{2} w_{rm} (\lambda_d i_q - \lambda_q i_d) \quad (5.15)$$

Where P is the number of poles in the machine and w_{rm} is the rotor speed in mechanical radians per second. From this, the torque is given as,

$$P_{em} = \frac{3}{2}\frac{P}{2} (\lambda_d i_q - \lambda_q i_d) \quad (5.16)$$

Now in order to implement the winding equations derived earlier, they are to be written in a form that uses voltages as the input and currents as the output quantities.

The inputs for the simulation are the stator abc voltages, excitation voltage and the applied mechanical torque to the rotor.

The transformation of the abc to qd0 reference frame for the stator voltages yields,

$$v_q = {v_q}^s \cos\theta_r(t) - {v_d}^s \sin\theta_r(t)$$

$$v_d = {v_q}^s \sin\theta_r(t) + {v_d}^s \cos\theta_r(t) \tag{5.17}$$

Here, the relation for $\theta_r(t) = \int_0^t w_r\,(t)dt + \theta_r(0)$ in electrical radians.

Using the relations for ${v_q}^s$ and ${v_d}^s$, we get,

$$v_q = \frac{2}{3}\{v_a \cos\theta_r(t) + v_b \cos\left(\theta_r(t) - \frac{2\pi}{3}\right) + v_c \cos\left(\theta_r(t) - \frac{4\pi}{3}\right)\}$$

$$v_d = \frac{2}{3}\{v_a \sin\theta_r(t) + v_b \sin\left(\theta_r(t) - \frac{2\pi}{3}\right) + v_c \sin\left(\theta_r(t) - \frac{4\pi}{3}\right)\}$$

$$v_0 = \frac{1}{3}(v_a + v_b + v_c) \tag{5.18}$$

The qd0 voltage equations can be expressed as integral equations of the flux linkages of the windings, such that they can be used to solve for the flux linkages, which are expressed as,

$$\psi_q = w_b \int\{v_q - \frac{w_r}{w_b}\psi_d + \frac{r_s}{x_{ls}}(\psi_{mq} - \psi_q)\}\,dt$$

$$\psi_d = w_b \int\{v_d + \frac{w_r}{w_b}\psi_q + \frac{r_s}{x_{ls}}(\psi_{md} - \psi_d)\}\,dt$$

$$\psi_0 = w_b \int\{v_0 - \frac{r_s}{x_{ls}}\psi_0\}\,dt \tag{5.19}$$

Where ψ_{mq} and ψ_{md} are the mutual flux linkages of the d and q axes, which when expressed in terms of the total flux linkages, can be given as,

$$\psi_{mq} = x_{MQ}\left(\frac{\psi_q}{x_{ls}} + \frac{\psi_{kq}{}'}{x_{lkq}{}'}\right)$$

$$\psi_{mq} = x_{MQ}\left(\frac{\psi_d}{x_{ls}} + \frac{\psi_{kd}{}'}{x_{lkd}{}'} + \frac{\psi_f{}'}{x_{lf}{}'}\right) \tag{5.20}$$

Where,

$$\frac{1}{x_{MQ}} = \frac{1}{x_{mq}} + \frac{1}{x_{lkq}{}'} + \frac{1}{x_{ls}}$$

$$\frac{1}{x_{MD}} = \frac{1}{x_{md}} + \frac{1}{x_{lkd}{}'} + \frac{1}{x_{lf}{}'} + \frac{1}{x_{ls}} \tag{5.21}$$

The winding currents can be thus determined as,

$$i_q = \frac{\psi_q - \psi_{mq}}{x_{ls}}$$

$$i_d = \frac{\psi_d - \psi_{md}}{x_{ls}} \quad (5.22)$$

The torque expression of eqn can also be rewritten as,

$$P_{em} = \frac{3}{2}\frac{P}{2w_b}(\psi_d i_q - \psi_q i_d) \quad (5.23)$$

This value of torque is taken positive for motoring operation, while it is treated negative for the generating convention.

For the rotor assembly, considering the motoring convention, the net acceleration torque, $T_{em} + T_{mec\,h} - T_{damp}$, is considered in the direction of the rotor's rotation. Equating this net accelerating torque to the inertial torque,

$$T_{em} + T_{mec\,h} - T_{damp} = J\frac{dw_{rm}(t)}{dt} = \frac{2J}{P}\frac{dw_r(t)}{dt} \quad (5.24)$$

The rotor angle, δ, is expressed as the angular difference between the rotor's position in the rotor reference frame and the synchronously rotating reference frame,

$$\delta(t) = \theta_r(t) - \theta_e(t) \quad (5.25)$$

The slip speed is given by the relation,

$$w_r(t) - w_e = \frac{P}{2J}\int_0^t (T_{em} + T_{mec\,h} - T_{damp})dt \quad (5.26)$$

The corresponding equations in the transient and subtransient conditions are given below.

The Stator winding relations are,

$$v_q = -ri_q + E_q'' - w_r L_d'' i_d + \frac{d_q}{dt} \quad (5.27)$$

$$v_d = -ri_d + E_d'' - w_r L_q'' i_q + \frac{d_d}{dt} \quad (5.28)$$

Where,

$$E_q'' = \left(\frac{L_d'' - L_{ls}}{L_d' - L_{ls}}\right)E_q' + \left(\frac{L_d' - L_d''}{L_d' - L_{ls}}\right)w_r \lambda_{kd}'$$

$$E_d{}'' = \left(\frac{L_q{}'' - L_{ls}}{L_q{}' - L_{ls}}\right) E_d{}' + \left(\frac{L_q{}' - L_q{}''}{L_q{}' - L_{ls}}\right) w_r \lambda_{kq}{}'$$

The rotor winding relations in terms of the torque are given as,

$$T_{d0}{}' \frac{dE_q{}'}{dt} =$$

$$E_f - w_r \left\{\frac{(L_d - L_d{}')(L_d{}'' - L_{ls})}{(L_d{}' - L_{ls})}\right\} i_d - \left\{1 + \frac{(L_d{}' - L_d{}'')(L_d - L_d{}')}{(L_d{}' - L_{ls})^2}\right\} E_q{}' + \left\{\frac{(L_d{}' - L_d{}'')(L_d - L_d{}')}{(L_d{}' - L_{ls})^2}\right\} w_r \lambda_{kd}{}' \quad (5.29)$$

$$T_{q0}{}' \frac{dE_d{}'}{dt} =$$

$$-E_g + w_r \left\{\frac{(L_q - L_q{}')(L_q{}'' - L_{ls})}{(L_q{}' - L_{ls})}\right\} i_q - \left\{1 + \frac{(L_q{}' - L_q{}'')(L_q - L_q{}')}{(L_q{}' - L_{ls})^2}\right\} E_d{}' + \left\{\frac{(L_q{}' - L_q{}'')(L_q - L_d{}')}{(L_q{}' - L_{ls})^2}\right\} w_r \lambda_{kq}{}' \quad (5.30)$$

$$T_{d0}{}'' \frac{d_{kd}{}'}{dt} = \frac{E_q{}'}{dt} - \lambda_{kd}{}' - (L_d{}' - L_{ls}) i_d \quad (5.31)$$

$$T_{q0}{}'' \frac{d_{kq}{}'}{dt} = \frac{E_d{}'}{dt} - \lambda_{kq}{}' - (L_q{}' - L_{ls}) i_q \quad (5.32)$$

The electromagnetic torque is given by,

$$T_{em} = -\frac{3}{2}\frac{P}{2}\left\{\left(\frac{E_q{}'' i_q + E_d{}'' i_d}{w_r}\right) + \left(L_q{}'' - L_q{}''\right) i_d i_q\right\} Nm \quad (5.33)$$

Simplifying,

$$T_{em} = -\left\{\left(\frac{E_q{}'' i_q + E_d{}'' i_d}{w_r / w_b}\right) + w_b \left(L_q{}'' - L_q{}''\right) i_d i_q\right\} Nm \quad (5.34)$$

5.1.2 Lumped Mass model

The shaft of a turbine generator is a complex mechanical assembly of several shaft sections with a large number of torsional modes of vibration. Although the complex shaft assembly can be represented by a continuum model in which the shaft might be subdivided into minute cylindrical sections, it is understood from previous experiences that when the torsional modes are below the synchronous frequency, a simpler lumped mass model representation is sufficient. The generally used model represents the individual sections connected using weightless springs.

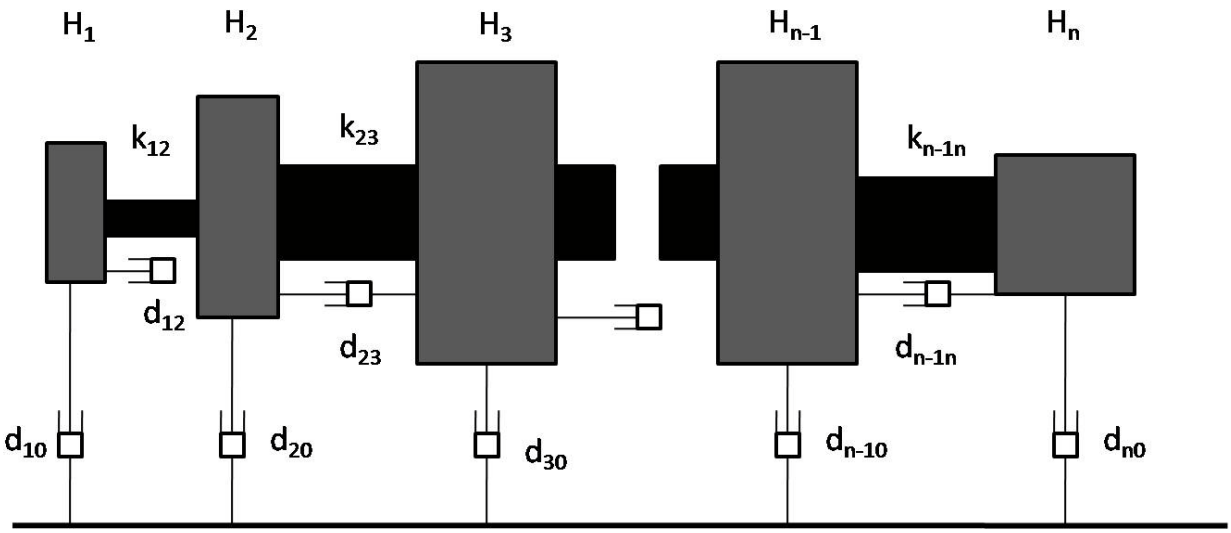

Fig 5.2 Lumped mass model

The various turbine sections can be mathematically represented by an equivalent mass spring system with their inertia, spring constant and damping. The mechanical system of the generator and exciter can be represented in a similar fashion. Inertia is expressed in terms of inertia constant H based on rated KVA. The simple second order torque equation in this system of units is:

$$\frac{2}{w_b} H\ddot{\delta} + D\dot{\delta} + K\delta = T \tag{5.35}$$

Where δ is the vector of the angular displacements or twists of the individual disk to a common reference, in electrical degrees. Here δ is positive in the direction of rotation of the shaft, and for convenience of expressing the terms in Kδ, δ is measured with respect to the first disk in the order that above equation is written, such that $\delta_1 = 0$. The base angular frequency is wb. The externally applied torques are given by the vector T, while H is a diagonal matrix whose elements are the inertia constants of the disks, such that H = diag (H_1, H_2, … H_n).

If the angle of the first disk is taken as the reference, the stiffness matrix, K, can be stated as:

$$\begin{bmatrix} k_{11} & \cdots & k_{1n} \\ \vdots & \ddots & \vdots \\ k_{n1} & \cdots & k_{nn} \end{bmatrix} \tag{5.36}$$

Where, in generic terms, k_{ij} is the torsional stiffness or spring constant of the portion of the shaft connecting masses i and j. It is based on the modulus of rigidity of the material, the section modulus, and the length of that portion of the shaft.

To represent the torsional damping between the masses, we use a damping coefficient D, given by the matrix:

$$\begin{bmatrix} d_{12} + d_{10} & \cdots & \\ \vdots & \ddots & \vdots \\ & \cdots & d_{nn} \end{bmatrix} \tag{5.37}$$

Where d_{i0} is the viscous damping of the i^{th} disk to the synchronously rotating reference frame, and d_{ij} is the viscous damping between the i^{th} and the j^{th} disks.

When considered without the effect of damping, the shaft assembly relation reduces to,

$$\frac{2}{w_b} H\ddot{\delta} + K\delta = T \tag{5.38}$$

Or

$$\ddot{\delta} + \frac{w_b}{2} H^{-1} K\delta = \frac{w_b}{2} H^{-1} T \tag{5.39}$$

The matrix based term, $\frac{w_b}{2} H^{-1}$, is defined as the torsional system matrix, which is a non-symmetrical tri-diagonal matrix. Assuming Harmonic motion and ignoring the excitation term, the natural (unforced) system becomes,

$$\left[\frac{w_b}{2} H^{-1} K - \lambda I\right] \delta = 0 \tag{5.40}$$

The characteristic equation is thus the determinant of the matrix equated to zero. The roots of the characteristic equation are known as the eigenvalues, which are the square of the natural frequencies of the system, w_{mi}.

It is to be noted that since the entire shaft assembly rotates as a solid body, it can be called a semidefinite system, which are characterized by one or more of the shaft's natural frequencies being equal to zero. For the above case, the mode with the zero natural frequency can be called the zero mode of the system. Thus, when n disks are connected by (n-1) flexible shaft sections, there will be (n-1) other modes of torsional modes of oscillations besides the zero mode.

By substituting λ_i into the natural system equation, we can solve to get the right eigenvector or mode shape vector, δ_{mi}

$$\left[\frac{w_b}{2} H^{-1}K - \lambda_i I\right]\delta_{mi} = 0$$

$$\frac{2\lambda_i}{w_b} H\delta_{mi} = K\delta_{mi} \tag{5.41}$$

Premultiplying by the transpose of the mode-shape vector, δ_{mj} , we have,

$$\delta_{mj}{}^t \frac{2\lambda_i}{w_b} H\delta_{mi} = \delta_{mj}{}^t K\delta_{mi} \tag{5.42}$$

Similar to the above, but interchanging the ith and jth modes, we get,

$$\delta_{mi}{}^t \frac{2\lambda_i}{w_b} H\delta_{mj} = \delta_{mi}{}^t K\delta_{mj} \tag{5.43}$$

As both the H and K matrices are known to be symmetric,

$$\delta_{mi}{}^t H\delta_{mj} = \delta_{mj}{}^t H\delta_{mi} \; and \; \delta_{mi}{}^t K\delta_{mj} = \delta_{mj}{}^t K\delta_{mi} \tag{5.44}$$

Subtracting Eq.5.34 from Eq.5.35 and using relations from Eq.5.36, we get,

$$\frac{2}{w_b}(\lambda_i - \lambda_j)\delta_{mj}{}^t H\delta_{mi} = 0 \tag{5.45}$$

As the eigenvectors are orthonormal, for λ_i not equal to λ_j ,

$$\delta_{mi}{}^t H\delta_{mj} = 0$$

And similarly,

$$\delta_{mi}{}^t K\delta_{mj} = 0$$

When i=j,

$$\delta_{mi}{}^{t} H \delta_{mj} = H_{mi}$$
$$\delta_{mi}{}^{t} K \delta_{mj} = K_{mi}$$

Where H_{mi} and K_{mi} are the generalized inertia and stiffness constants, respectively.

Let Q be a matrix whose columns denote the right eigenvectors of the matrix $H^{-1}K$, and it can be multiplied by an arbitrary constant, like,

$$S=QR$$

Where R is a scaling matrix that is diagonal and of the same order as Q. S or Q are often referred to as the modal matrix, because the n columns represent the modes of vibration of the n-disk system. Therefore, that corresponding to the frequency of zero is called mode 0, while that for the next higher frequency is called mode 1.

The transformation from actual to modal angles can be done by substituting $\delta = S\delta_m$. So after premultiplying the equation 10.124 by transpose of S matrix and using the above substitution, we get,

$$\frac{2}{w_b} S^T H S \ddot{\delta}_m + S^T D S \dot{\delta}_m + S^T K S \delta_m = S^T T \qquad (5.46)$$

In the above relation, we can rewrite the terms to make it more compact. So, $S^T H S = H_m$, $S^T D S = D_m$, $S^T K S = K_m$, and $S^T T = T_m$. The subscript m is used to denote the modal quantities. So it can now be given as,

$$\ddot{\delta}_m + \frac{w_b}{2} H_m{}^{-1} D_m \dot{\delta}_m + \frac{w_b}{2} H_m{}^{-1} K_m \delta_m = \frac{w_b}{2} H_m{}^{-1} S^T T_m \qquad (5.47)$$

Since the above are diagonal matrices, the equations of the modes can be decoupled from one another and have a form similar to that derived earlier. Comparing the form of the modal equations with the normal second order equation, we can identify that,

$$2\zeta_i w_{mi} = \frac{w_b}{2}\frac{D_{mi}}{H_{mi}} \quad (5.48)$$

Where ζ_i, the damping factor, is a dimensionless quanity. It is usually defined as the actual damping to the critical damping. So when ζ_i<<1, the response will be under-damped.

5.2 Network modeling

To model the transmission line in the system, Park's transformation is employed for both the series RL and shunt capacitance circuits.

5.2.1 Transmission Line

For the transmission line which is considered made up of RL components, let us denote the line resistances of the 3 phases to be r_a, r_b, r_c, while the line inductances are taken as L_{aa}, L_{bb}, L_{cc}. The mutual inductances are denoted as L_{ab}, L_{bc} and L_{ca}. Similarly, the ground resistance is taken as r_g, while the inductance is L_{gg}. The line to ground voltages of sending end are denoted by v_{asgs}, v_{bsgs} and v_{csgs}, while that of the receiving end are v_{argr}, v_{brgr} and v_{crgr}.

The sending end voltage with respect to local ground is given as,

$$v_{asgs} = i_a r_a + L_{aa}\frac{di_a}{dt} + L_{ab}\frac{di_b}{dt} + L_{ac}\frac{di_c}{dt} + L_{ag}\frac{di_g}{dt} + v_{argr} + v_{grgs} \quad (5.49)$$

Using the relation $i_g = -(i_a + i_b + i_c)$, the voltage drops across the three phase lines can be expressed in matrix form as,

$$[v_S] - [v_R] = [R][i] + \frac{d}{dt}[L][i] \quad (5.50)$$

Where,

$$[v_S] = \begin{bmatrix} v_{asgs} \\ v_{bsgs} \\ v_{csgs} \end{bmatrix};$$

$[v_R] = \begin{bmatrix} v_{argr} \\ v_{brgr} \\ v_{crgr} \end{bmatrix}$;

$[R] = \begin{bmatrix} r_a + r_g & r_g & r_g \\ r_g & r_b + r_g & r_g \\ r_g & r_g & r_c + r_g \end{bmatrix}$ and

$[L] = = \begin{bmatrix} L_{aa} + L_{gg} - 2L_{ag} & L_{ab} + L_{gg} - L_{bg} - L_{ag} & L_{ac} + L_{gg} - L_{cg} - L_{ag} \\ L_{ab} + L_{gg} - L_{ag} - L_{bg} & L_{bb} + L_{gg} - 2L_{bg} & L_{bc} + L_{gg} - L_{cb} - L_{bg} \\ L_{ca} + L_{gg} - L_{ag} - L_{cg} & L_{bc} + L_{gg} - L_{bg} - L_{cg} & L_{cc} + L_{gg} - 2L_{cg} \end{bmatrix}$

The voltage drops across the ground path is geiven by,

$$v_{grgs} = -v_{grgr} = -i_g r_g - L_{gg}\frac{di_g}{dt} - L_{ab}\frac{di_a}{dt} - L_{bg}\frac{di_b}{dt} - L_{cg}\frac{di_c}{dt}$$
$$= r_g(i_a + i_b + i_c) + \left(L_{gg} - L_{ag}\right)\frac{di_a}{dt} + \left(L_{gg} - L_{bg}\right)\frac{di_b}{dt} + (L_{gg} - L_{cg})\frac{di_c}{dt} \quad (5.51)$$

When we use a uniformly transposed line, $r_a = r_b = r_c$, $L_{ab} = L_{bc} = L_{ca}$ and $L_{ag} = L_{bg} = L_{cg}$. Assuming $L_s = L_{aa} + L_{gg} - 2L_{ag}$, $L_m = L_{ab} + L_{gg} - 2L_{ag} = L_s - L_{aa} + L_{ab}$, $r_s = r_a + r_g$ and $r_m = r_g$, the resistance and inductance matrixes get simplified to,

$$[R] = \begin{bmatrix} r_s & r_m & r_m \\ r_m & r_s & r_m \\ r_m & r_m & r_s \end{bmatrix} and\ [L] = \begin{bmatrix} L_s & L_m & L_m \\ L_m & L_s & L_m \\ L_m & L_m & L_s \end{bmatrix}$$

The qd0 equations for the uniformly transposed line can be arrived separately by taking into account the resistive and inductive drops of the phases. Let us first consider the a-phase resistive drop,

$$r_s i_a + r_m\,(i_b + i_c) \quad (5.52)$$

Substituting $i_0 = (i_a + i_b + i_c)/3$ to get in terms of only a-phase,

$$(r_s - r_m)i_a + 3r_m i_0 \quad (5.53)$$

Expressing ia in terms of the qd0 components, the resistive drop becomes,

$$(r_s - r_m)(i_q \cos\theta_q + i_d \sin\theta_d + i_0) + 3r_m i_0 \quad (5.54)$$

The inductive drop of the a-phase is given as,

$$L_s \frac{di_a}{dt} + L_m \frac{d(i_b + i_c)}{dt} \quad (5.55)$$

Again getting in terms of only a-phase current,

$$(L_s - L_m)\frac{di_a}{dt} + 3L_m \frac{di_0}{dt} \quad (5.56)$$

Writing in terms of the qd0 currents,

$$(L_s - L_m)\frac{d(i_q \cos\theta_q + i_d \sin\theta_d + i_0)}{dt} + 3L_m \frac{di_0}{dt} \quad (5.57)$$

Now applying the qd0 transformation to the voltage across the sending and receiving ends of the a-phase, and further equating the coefficients of the $\cos\theta_q, \sin\theta_q$, and constant terms, we obtain,

$$\frac{dv_q}{dt} = (r_s - r_m)i_q + (L_s - L_m)\frac{di_q}{dt} + (L_s - L_m)i_d \frac{d\theta_q}{dt}$$
$$\frac{dv_d}{dt} = (r_s - r_m)i_d + (L_s - L_m)\frac{di_d}{dt} - (L_s - L_m)i_q \frac{d\theta_q}{dt}$$
$$\frac{dv_0}{dt} = (r_s + 2r_m)i_0 + (L_s + 2L_m)\frac{di_0}{dt} \quad (5.58)$$

The corresponding voltage drop equation of the same line in the symmetrical components is given by,

$$\Delta\begin{bmatrix} v_0 \\ v_1 \\ v_2 \end{bmatrix} = \begin{bmatrix} z_s + 2z_m & & \\ & z_s - z_m & \\ & & z_s - z_m \end{bmatrix} \Delta\begin{bmatrix} i_0 \\ i_1 \\ i_2 \end{bmatrix} \quad (5.59)$$

The qd0 equations of the voltage drops across the line given in the original phase parameters of the line are,

$$(r_s - r_m) = r_a$$
$$(r_s + 2r_m) = (r_a + 3r_g)$$
$$(L_s - L_m) = (L_{aa} - L_{ab})$$
$$(L_s - L_m) = (L_{aa} + 2L_{ab}) + 3(L_{gg} - 2L_{ag}) \quad (5.60)$$

If we consider the mutual inductances between the phases and that between the phases and ground to be zero,

$L_{ab} = L_{bc} = L_{ac} = 0 \; and \; L_{ag} = L_{bg} = L_{cg} = 0$

Then, $L_s = L_{aa} + L_{gg}$ and $L_m = L_{gg}$

Assuming voltage input, the qd0 currents can be obtained by solving the below integral equations,

$$i_q = \frac{1}{L_{aa}} \int (v_{qs} - v_{qr} - wL_{aa} i_d - i_q r_a) dt$$

$$i_d = \frac{1}{L_{aa}} \int (v_{ds} - v_{dr} + wL_{aa} i_q - i_d r_a) dt$$

$$i_0 = \frac{1}{L_{aa} + 3L_{gg}} \int (v_{0s} - v_{0r} - i_0 r_a + 3r_g) dt \quad (5.61)$$

5.2.2 Shunt Capacitances

The shunt capacitors have been included in the model in order to develop the terminal voltages of the generator. Let the phase to neutral capacitances and the mutual capacitances between the phases be such that,

$C_{ab} = C_{bc} = C_{ca} = C_m; C_{an} = C_{bn} = C_{cn} \; and \; C_s = C_{an} + C_{ab}$

Thus, the equation of the a-phase current can be given as,

$$i_a = C_{an} \frac{dv_{an}}{dt} + C_{ab} \frac{d(v_{an} - v_{bn})}{dt} + C_{ac} \frac{d(v_{an} - v_{cn})}{dt} \quad (5.62)$$

Simplifying,

$$i_a = (C_{an} + C_{ab} + C_{ac}) \frac{dv_{an}}{dt} - C_m \frac{dv_{bn}}{dt} + C_m \frac{dv_{cn}}{dt} \quad (5.63)$$

By substituting to get in terms of only a-phase voltage,

$$i_a = (C_s + C_m) \frac{dv_{an}}{dt} - 3C_m \frac{dv_0}{dt} \quad (5.64)$$

Applying the qd0 transformation for both the current and voltage of the a-phase, we get,

$$i_q \cos\theta_q + i_d \sin\theta_q + i_0 = (C_s + C_m)\frac{d}{dt}\left(v_q \cos\theta_q + v_d \sin\theta_q + v_0\right) - 3C_m \frac{dv_0}{dt} \quad (5.65)$$

Equating the coefficients of the – and constant terms, the qd0 currents are obtained as,

$$i_q = (C_s + C_m)\frac{dv_q}{dt} + (C_s + C_m)v_d w$$

$$i_q = (C_s + C_m)\frac{dv_q}{dt} + (C_s + C_m)v_d w$$

$$i_0 = (C_s - 2C_m)\frac{dv_0}{dt} \quad (5.66)$$

Therefore, writing in terms of the original capacitance parameters,

$$(C_s + C_m) = (C_{an} + 3C_{ab})$$

$$(C_s - 2C_m) = (C_{an}) \quad (5.67)$$

The voltage equations in the integral form are given by,

$$v_q = \frac{1}{(C_s + C_m)}\int (i_q - (C_s + C_m)v_d \frac{d\theta_q}{dt})dt$$

$$v_d = \frac{1}{(C_s + C_m)}\int (i_d + (C_s + C_m)v_q \frac{d\theta_q}{dt})dt$$

$$v_0 = \frac{1}{(C_s - 2C_m)}\int i_0 dt \quad (5.68)$$

5.3 Composite model

A radial network is used to connect the generator and the infinite bus. Though the entire system is represented in the rotor reference frame, the infinite bus voltage components have been given in the synchronously rotating reference frame, and therefore they are converted to the rotor referenced rotating frame using the following transformation,

$$v_q = {v_q}^e \cos\delta - {v_d}^e \sin\delta$$

$$v_d = {v_q}^e \sin\delta + {v_d}^e \cos\delta \quad (5.69)$$

The composite SIMULINK model based on the relations derived earlier in this chapter is shown in figure 5.4

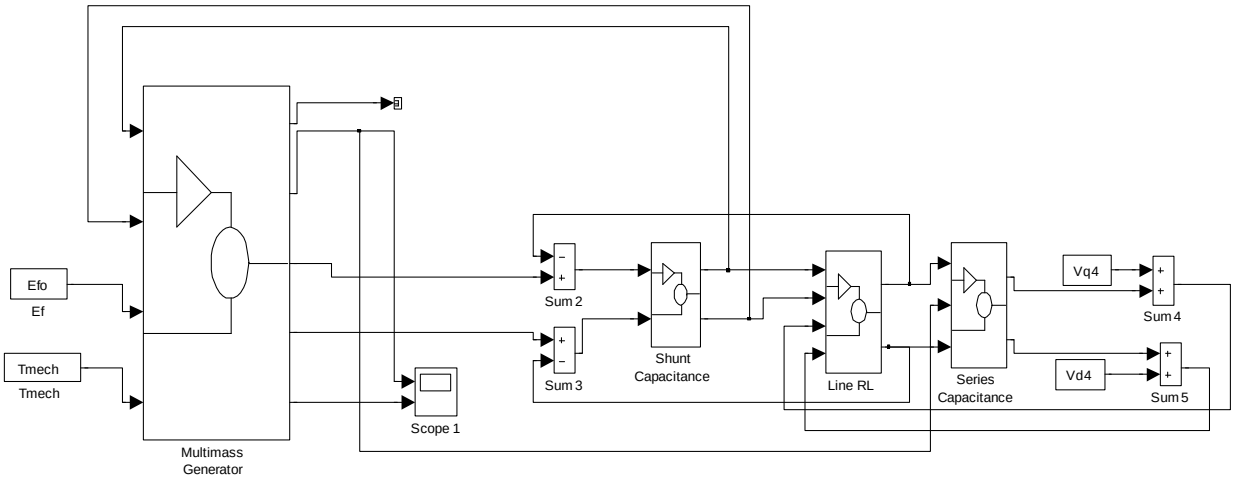

Fig 5.4 SIMULINK model of the test system

The generator and related masses (rotor, turbines, exciter) are represented by a multimass model, which has the excitation voltage and stator voltage components as its inputs. The block has internal elements that convert the parameters from the stator reference frame to that of the rotor, and also generate the torque, current and speed deviation signals.

The Shunt capacitances block uses q and d components of currents as its inputs, and is followed by the line reactance block, which uses corresponding voltage components as its inputs. The series capacitance block that follows this is used to model the effective series capacitive reactance in the system, and based on the application, the configuration may be altered, as will be seen in the following chapter.

CHAPTER 6

CASE STUDIES AND RESULTS

The IEEE first benchmark model parameters are loaded into the SIMULINK model developed in chapter 5 through a separate MATLAB program.

As per equation 2.4, the mechanical resonant frequency is derived as a complement of the electrical frequency. For the system in consideration, there are 5 modes of resonance, with corresponding frequencies of 15.71 Hz, 20.21 Hz, 25.55 Hz, 32.28 Hz and 47.45 Hz.

The total inductive reactance, comprising of generator, line and transformer reactance, is given to be 0.8675 p.u. A capacitive compensation of 0.473 p.u. is added to the system. The corresponding electrical resonant frequency is given from equation as:

$$f_e = f_0 \sqrt{\frac{X_C}{X_{LT}}}$$

$$f_e = 60 \sqrt{\frac{0.473}{0.8675}}$$

$$f_e = 44.31\ Hz$$

Thus the complement of this electrical resonant frequency is 15.69 Hz, close to 15.71 Hz mode that can excite SSR oscillations.

6.1 Simulation of SSR

In order to simulate the SSR phenomenon, first a fixed capacitor of value 0.473 pu is incorporated in series with the transmission line of the system. The results of the speed deviation and the LPA-LPB torque are given in figure 6.1

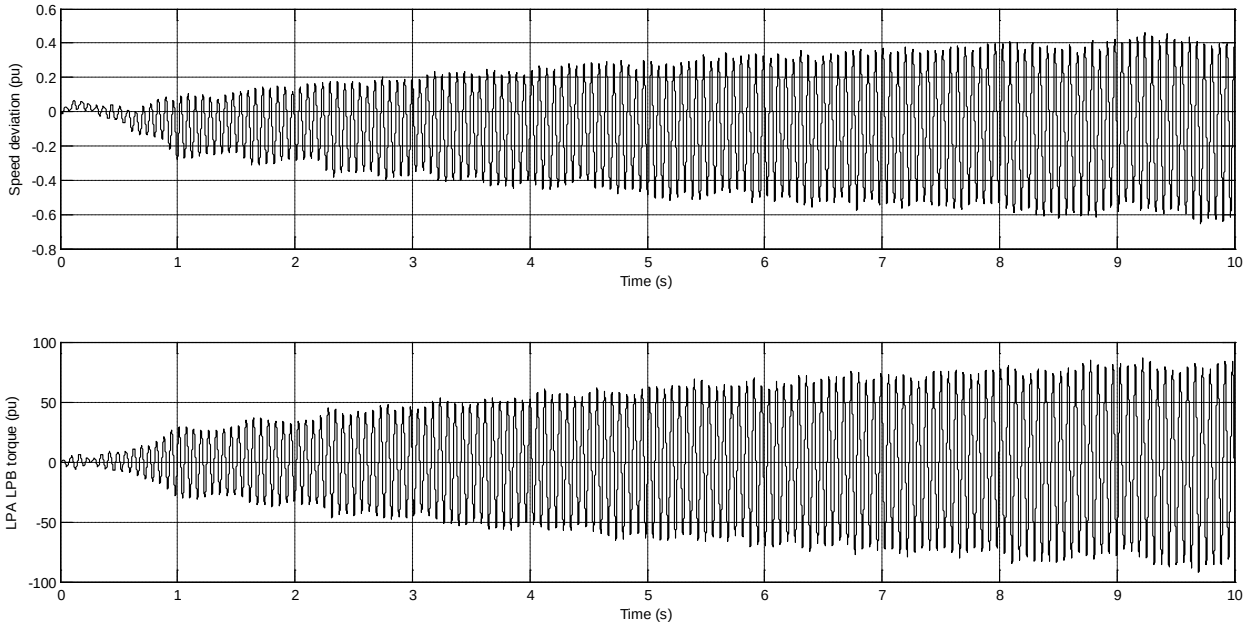

Fig 6.1 Simulation of SSR phenomenon

6.2 System with PSS

In order to mitigate the occurrence of SSR, a PSS is devised with the shaft speed variation as the input signal.

The main components of the PSS are:

1) Washout circuit for reset action to eliminate steady offset. T_w can range from 0.5 to 10 seconds.
2) Phase compensation stages
3) Appropriate gain stage

The system incorporating the PSS is shown in figure 6.2

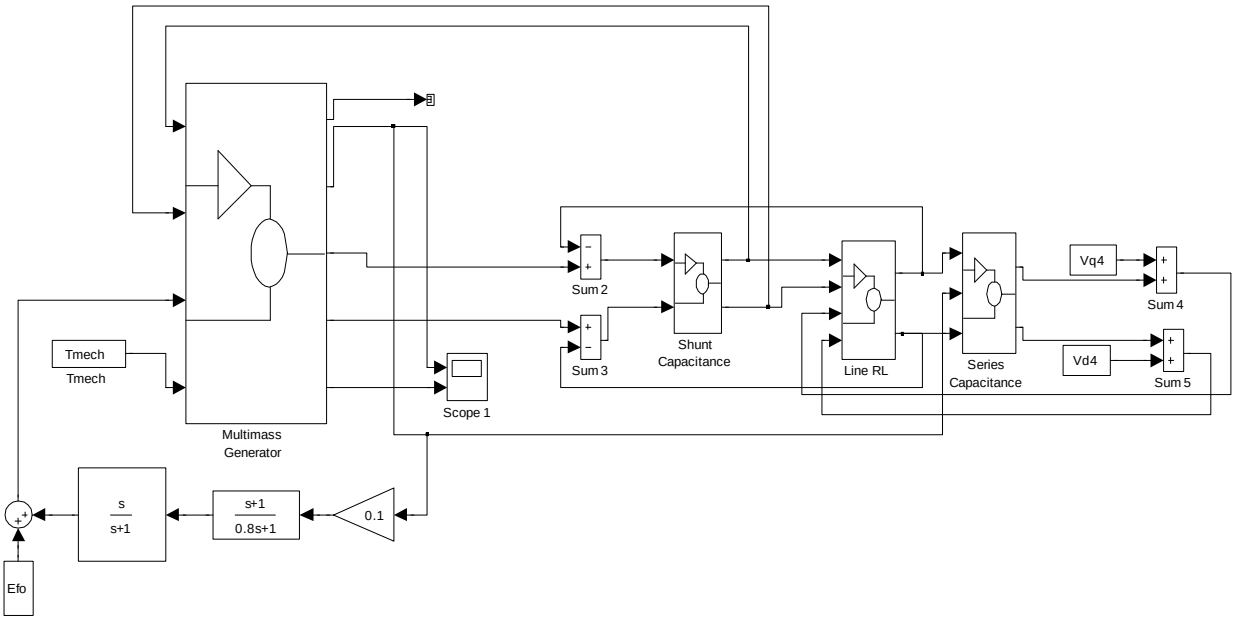

Fig 6.2 System with PSS

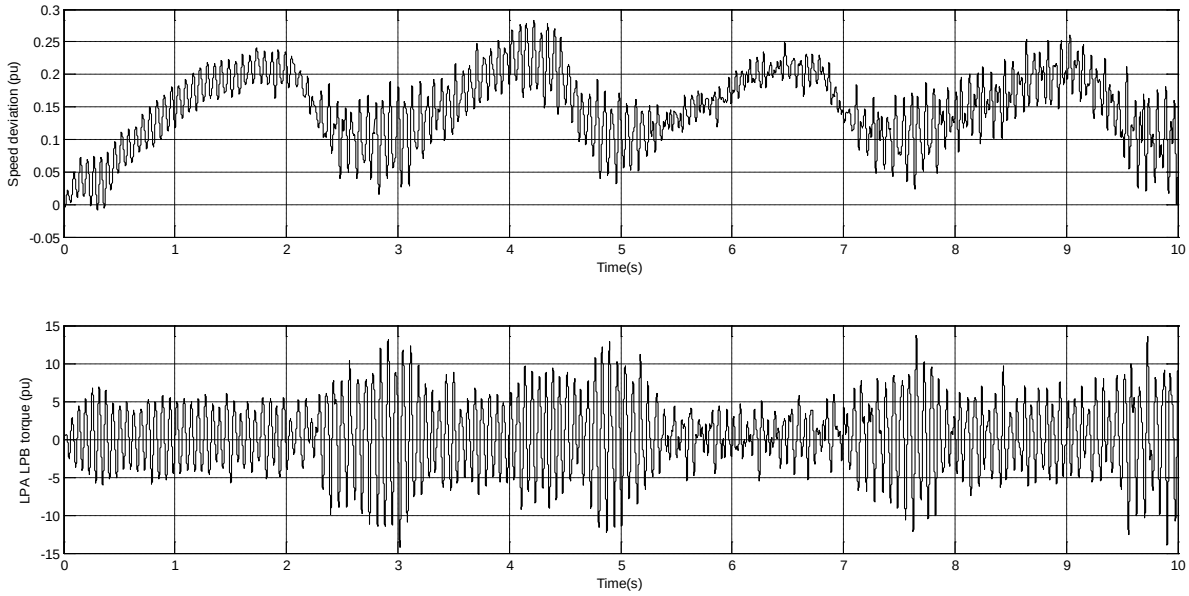

Fig 6.3 Results with PSS

The results with the PSS show a marginal improvement in the response of the system, but oscillations still persist at various points and are not completely quenched. Thus, we move on to implementing a variable capacitive reactance (TCSC) based on the reactance relation given by equation 4.17

6.3 System with TCSC

The fixed capacitor is replaced with a variable capacitive reactance based on the formula of the TCSC reactance derived in chapter 4. The initial firing angle is kept at a constant value of 152º, such that the effective reactance is capable of exciting the 15.71 Hz subsynchronous mode. To mitigate this, a feedback signal is given such that the net conduction angle is modulated, and hence the effective reactance does not lead to SSR in the system.

The series capacitance block which is modified to incorporate the TCSC variable reactance is shown in figure 6.4.

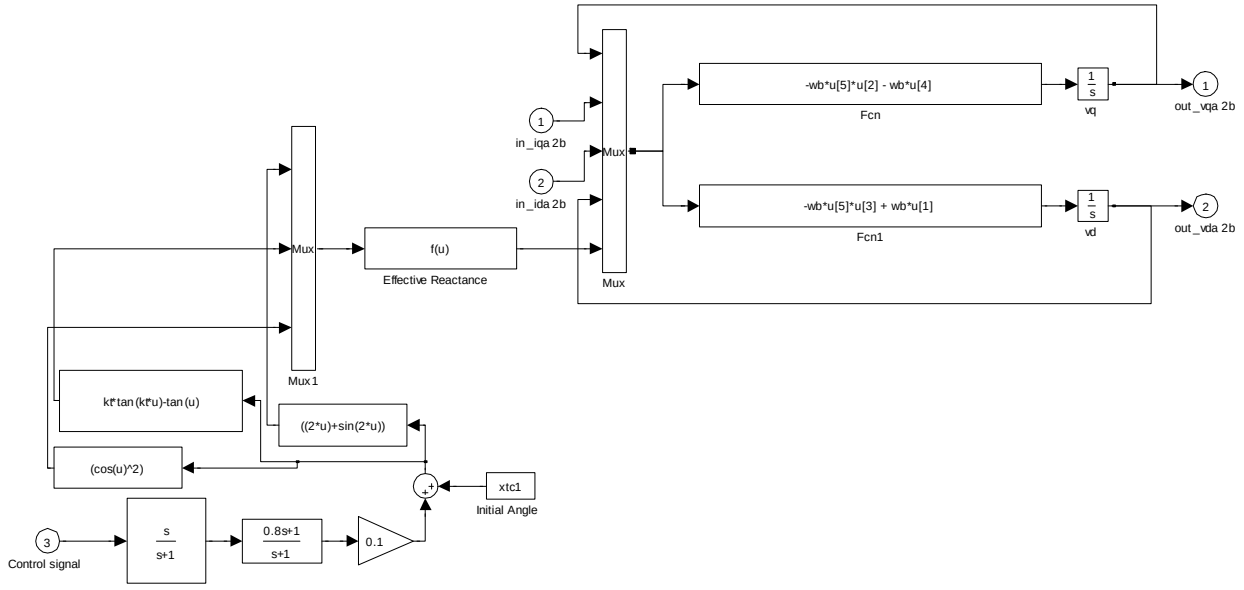

Fig 6.4 TCSC Reactance configuration

Various cases are analyzed with separate feedback signals – shaft speed variation and line current. Corresponding parameters of the feedback loop are varied in order to achieve optimum results, and they are given sequentially in the following pages.

TCSC capacitive reactance with positive speed feedback

Case Study 1:

Controller parameters

Gain: 0.1

Washout - Tw1: 1

Phase compensation stages - Tw2: 0.2, Tw3: 1

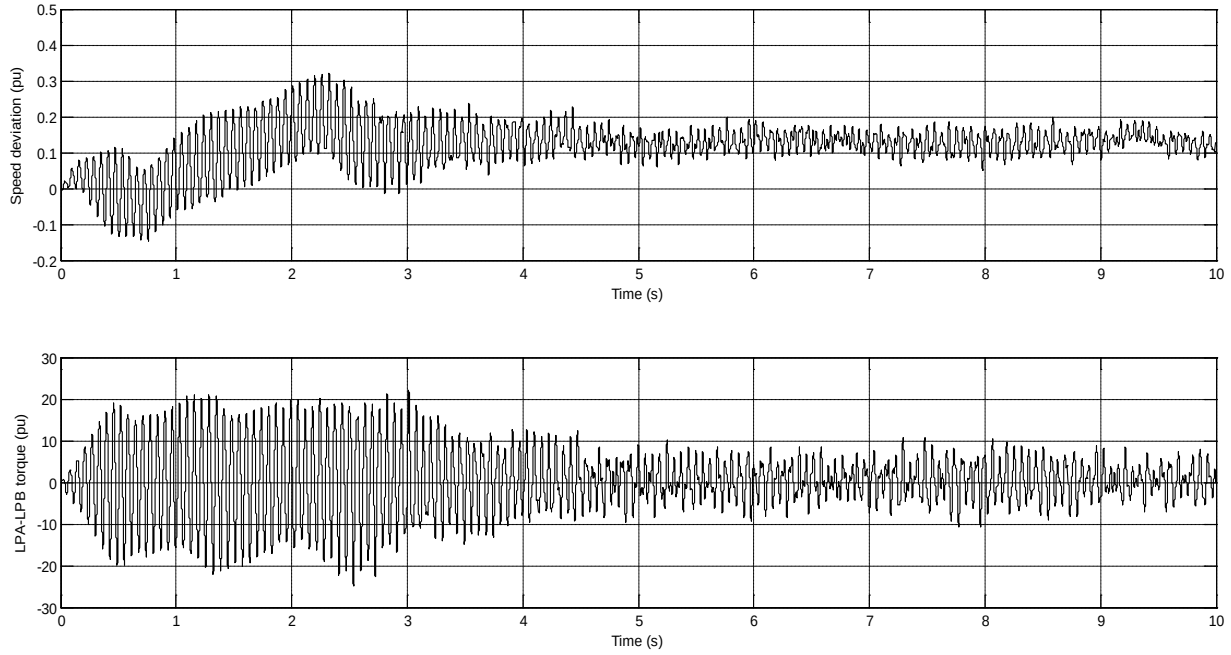

Fig 6.5 Results with TCSC (speed feedback) case study 1

Case Study 2:

Controller parameters

Gain: 0.1

Washout - Tw1: 1

Phase compensation stages - Tw2: 0.6, Tw3: 1

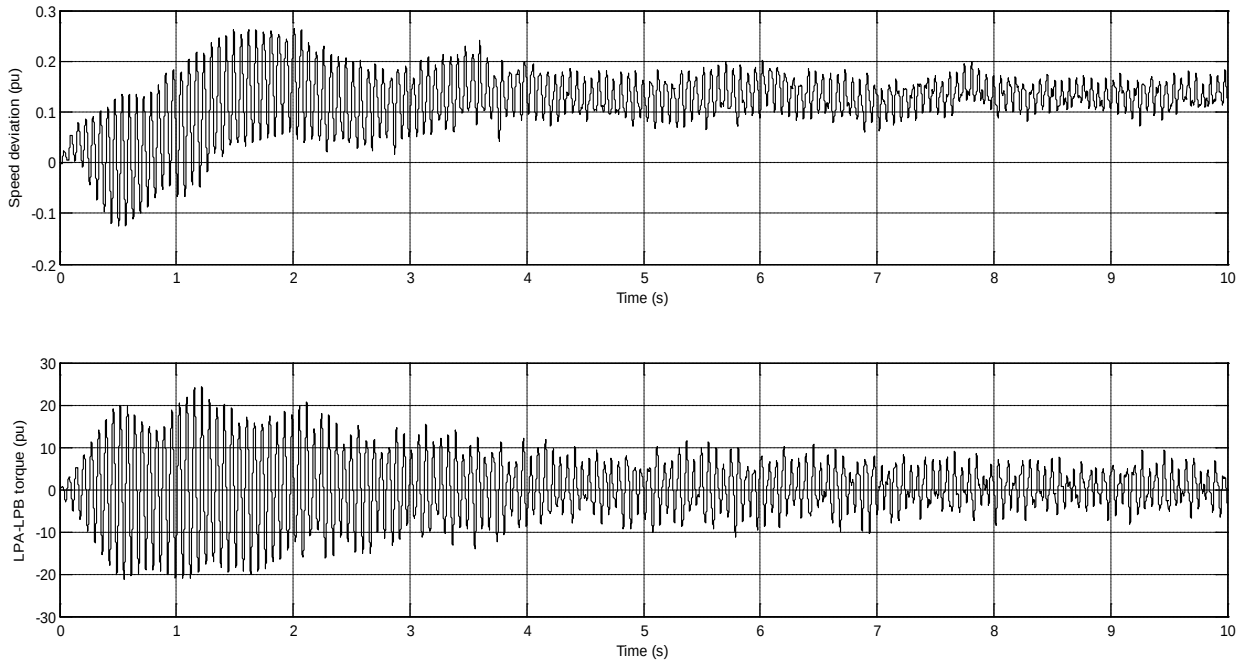

Fig 6.6 Results with TCSC (speed feedback) case study 2

Case Study 3:

Controller parameters

Gain: 0.1

Washout - Tw1: 1

Phase compensation stages - Tw2: 1, Tw3: 0.8

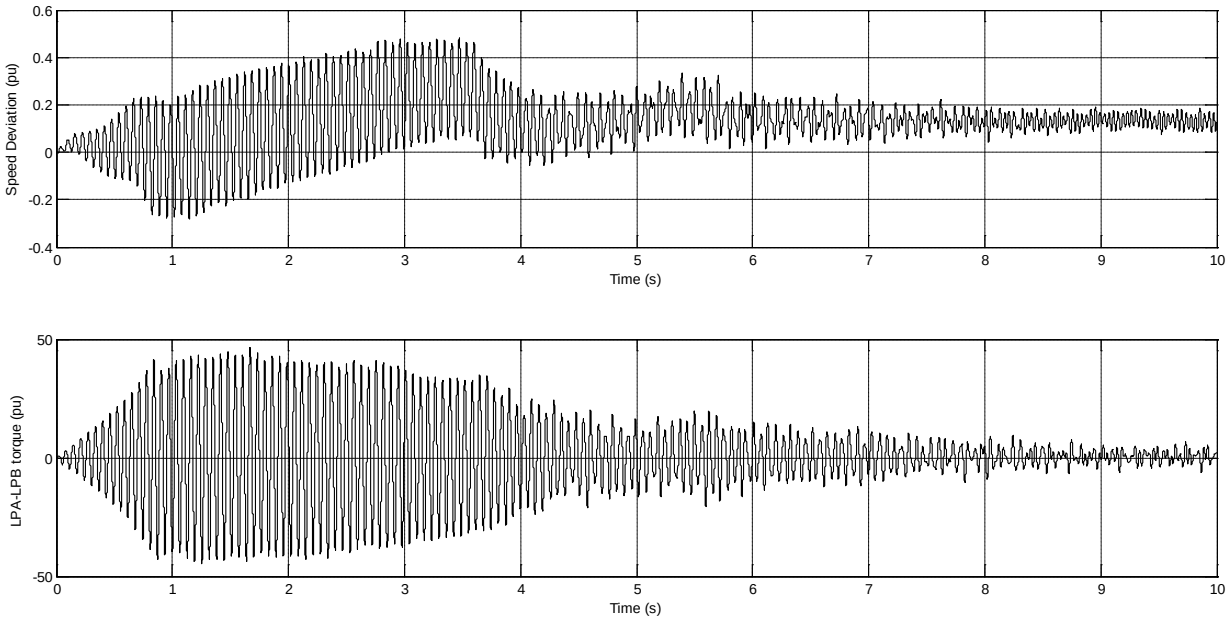

Fig 6.7 Results with TCSC (speed feedback) case study 3

TCSC capacitive reactance with negative current feedback

Case Study 1:

Controller parameters

Gain: 0.001

Washout - Tw1: 1

Phase compensation stages - Tw2: 1, Tw3: 0.4

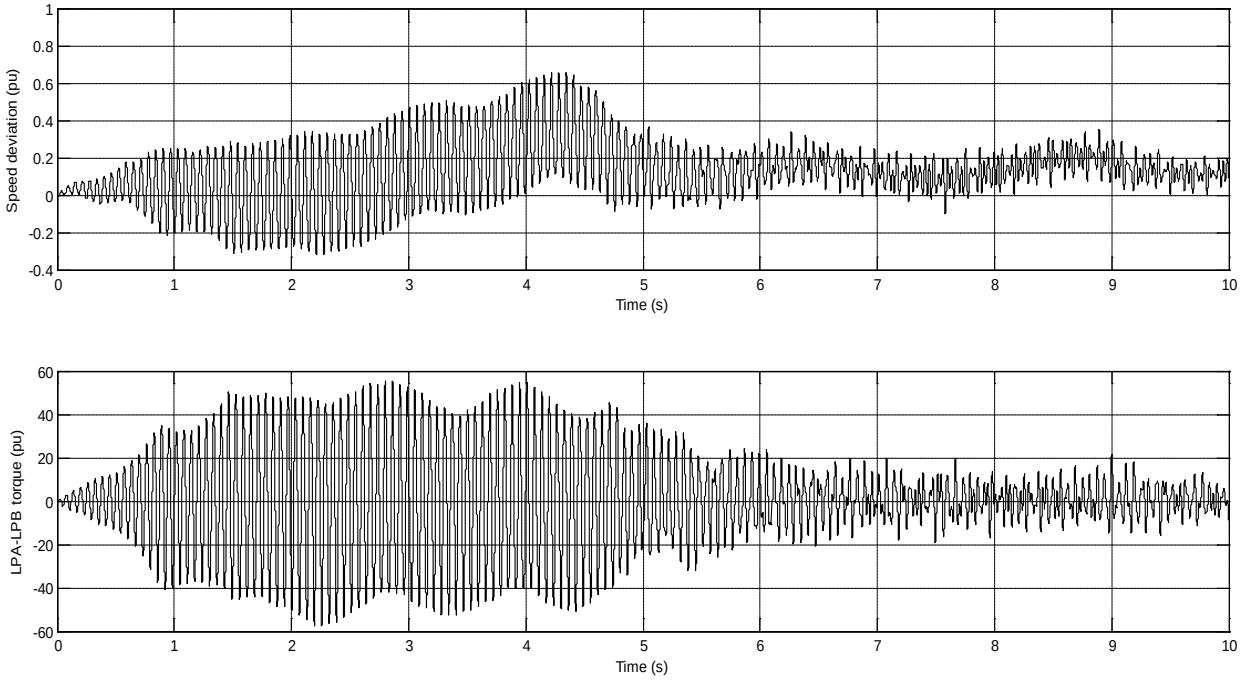

Fig 6.8 Results with TCSC (current feedback) case study 1

Case Study 2:

Controller parameters

Gain: 0.1

Washout - Tw1: 1

Phase compensation stages - Tw2: 0.6, Tw3: 1

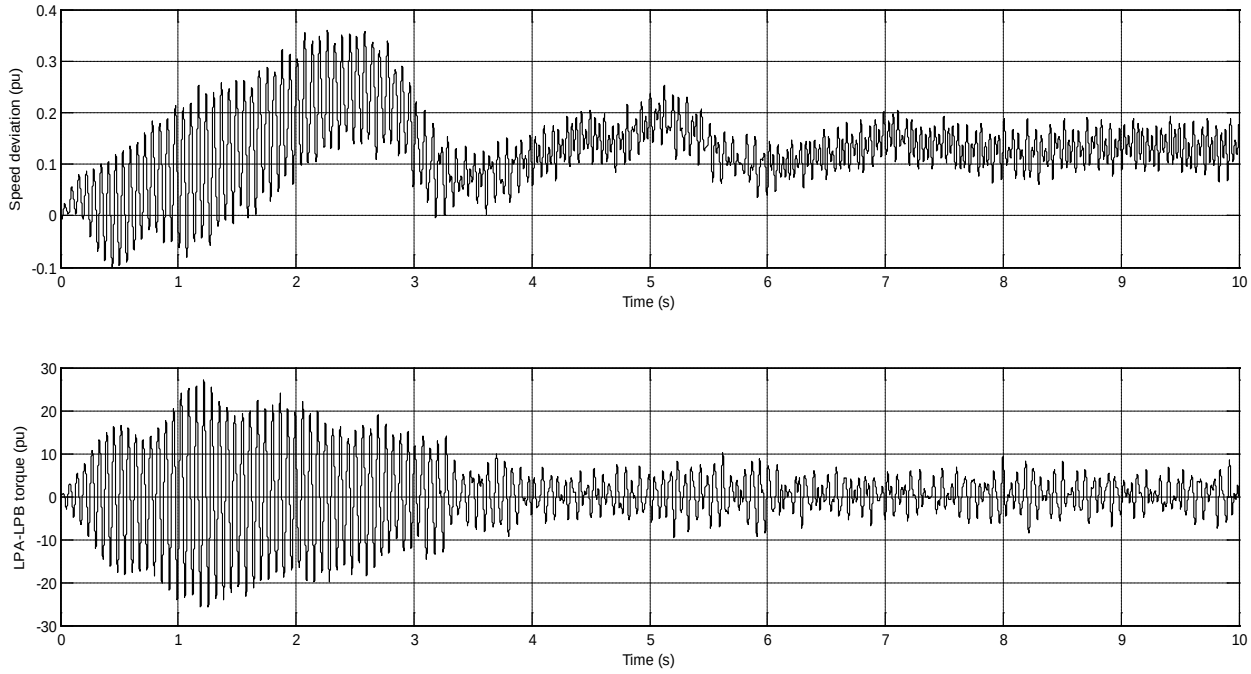

Fig 6.9 Results with TCSC (current feedback) case study 2

Case Study 3:

Controller parameters

Gain: 0.1

Washout - Tw1: 1

Phase compensation stages - Tw2: 0.2, Tw3: 1

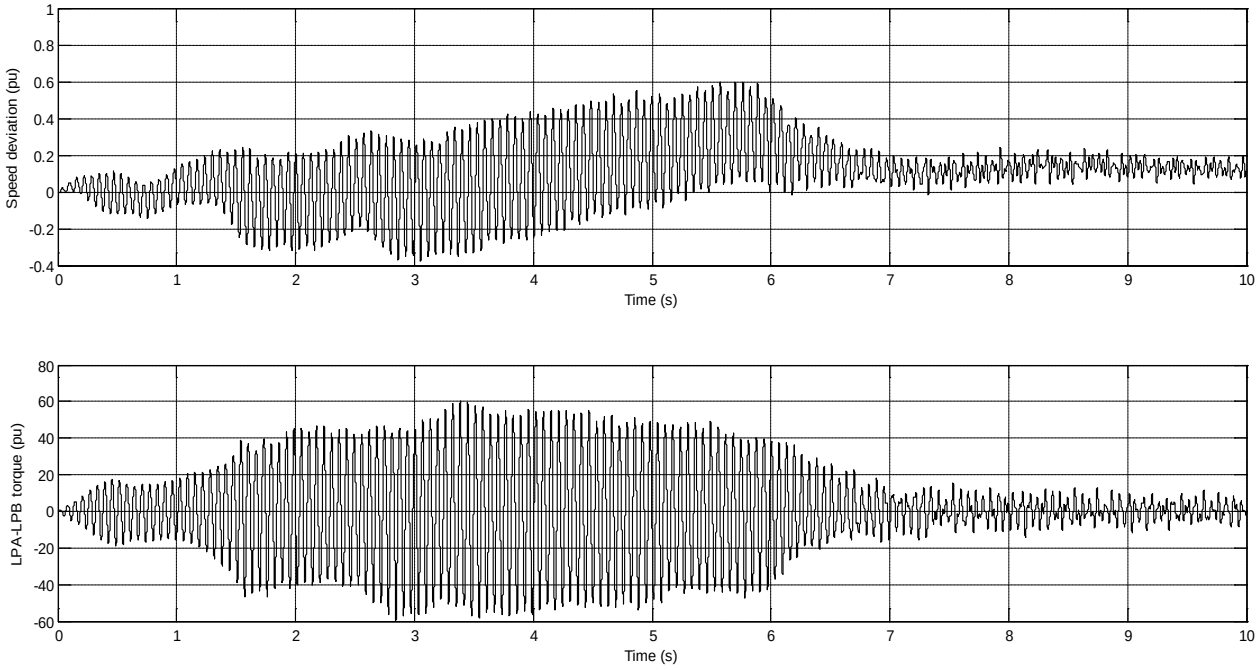

Fig 6.10 Results with TCSC (current feedback) case study 3

From the above cases of using a TCSC as a variable reactance, it is seen that the SSR phenomenon is sufficiently quenched. Though the intermediate oscillations are seen to be more in the case of the current being used as a feedback signal, as the speed deviation might not be readily available for use as the supplementary signal, a trade-off has to be made for the same.

6.4 System with PSS and TCSC

Finally, the effect of a TCSC in conjunction with a PSS is observed, and it is seen that the results are quite similar to that of using only the TCSC. From this it can be inferred that the effect of a TCSC in mitigating the SSR phenomenon is superior as compared to the PSS.

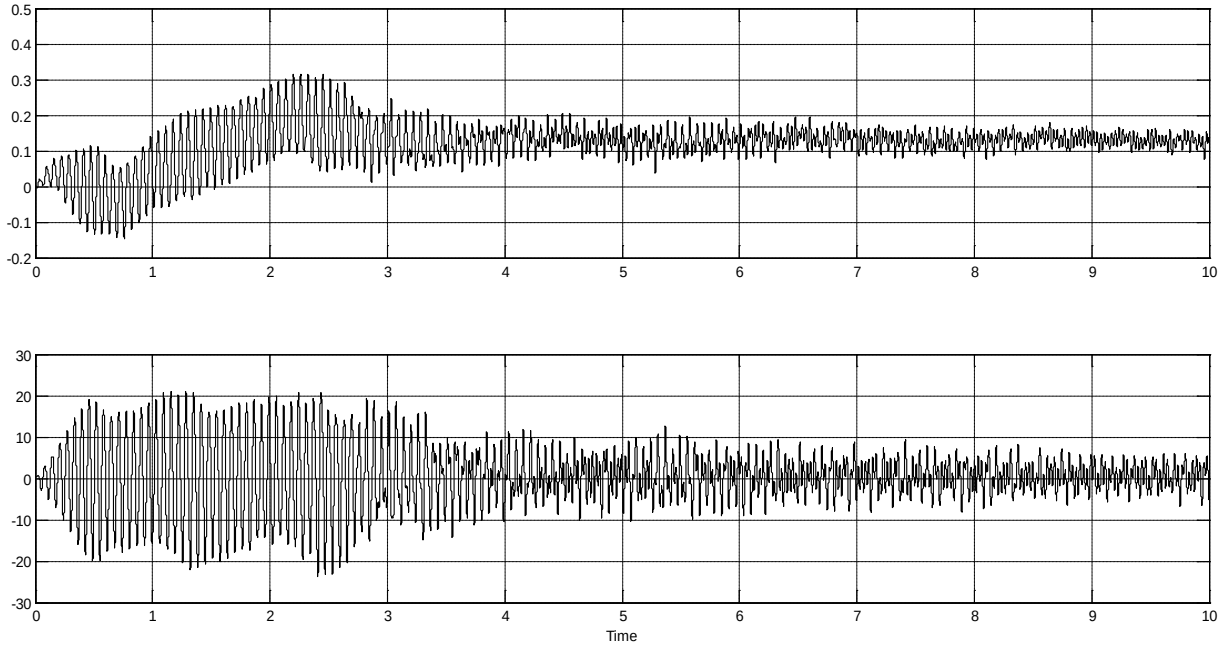

Fig 6.11 Results with TCSC and PSS

CHAPTER 7

CONCLUSIONS AND SCOPE FOR FURTHER WORK

In this work, a SIMULINK model is developed in order to analyze and then quench subsynchronous resonance (SSR), a potentially fatal phenomenon prevalent in power systems due to series compensation. Initially a Power system stabilizer (PSS) is devised for this purpose, which is seen to yield limited positive results. Subsequently, a Thyristor-controlled series capacitor (TCSC) was developed for the same. Case studies performed with the IEEE first benchmark model with different supplementary control signals demonstrate substantial SSR mitigation, and establish the effectiveness of a TCSC in overcoming the SSR phenomenon while being a capable device for the enhancement of power transmission levels.

With the advancements in the field of power electronics controllers, this work can be expanded in order to achieve more optimal results by working towards an advanced firing angle control model of the TCSC in the future.

REFERENCES:

[1] P. Kundur, Power system stability and control, New York: McGraw-Hill, 1994.

[2] J.W. Butler and C. Concordia, “Analysis of Series Capacitor Application Problems,” IEEE Transactions, Vol.56, 1937, pp.975-988.

[3] D. Walker, C. Bowler, R. Jackson, and D. Hodges, “Results of subsynchronous resonance test at Mohave,” IEEE Transactions on Power Apparatus and Systems, vol. 94, no. 5, pp. 1878–1889, 1975.

[4] IEEE SSR Task Force, “First Benchmark Model for Computer Simulation of Subsynchronous Resonance”, IEEE Trans. on PAS, Vol. PAS-96, pp. 1565-1572, Sept.-Oct. 1977.

[5] IEEE SSR Working Group, “Second Benchmark Model for Computer Simulation of Subsynchronous Resonance”, IEEE Trans. on PAS, Vol. PAS-104, pp. 1057-1066, May 1985.

[6] D.J.N.Limebeer, R.G.Harley, M.A.Lahoud, "Suppressing subsynchronous resonance with static filters," Generation, Transmission and Distribution, IEE Proceedings , vol.128, no.1, pp.33-44, January 1981

[7] IEEE SSR Working Group, "Countermeasures to subsynchronous resonance problems," IEEE Trans. Power App. Syst., vol. PAS-99, pp. 1810-1818, Sep. 1980.

[8] M. R. Iravani and R. M. Mathur, “Damping subsynchronous oscillations in power systems using a static phase-shifter,” IEEE Trans. Power Syst., vol. 1, no. 2, pp. 76–82, May 1986.

[9] P.Kundur, M.Klein, G.J. Rogers, M.S. Zywno, “Application of power system stabilizers for enhancement of overall system stability”, IEEE Trans. Power Systems, Vol.4, No.2, May 1989.

[10] Fan Zhang and Zheng Xu, "Effect of exciter and PSS on SSR damping," in Proc. IEEE PES General Meeting, June 2007, pp. 1-7.

[11] K. R. Padiyar, Power System Dynamics: Stability and Control, B.S. Publications, Hyderabad, India, 2nd edition, 2000.

[12] A. H. M. A. Rahim, A. M. Mohammad, and M. R. Khan, “Control of subsynchronous resonant modes in a series compensated system through superconducting magnetic energy storage units,” IEEE Trans. Energy Convers., vol. 11, no. 1, pp. 175–180, Mar. 1996.

[13] S.K. Gupta, Narendra Kumar, A.K. Gupta, ”Damping subsynchronous resonance in power systems”, IEE Proc. on Generation, Transmission, and Distribution, vol. 149, No.6, pp. 679-688, Nov. 2002.

[14] S. Purushothaman, “Eliminating Subsynchronous oscillations with an Induction Machine Damping Unit(IMDU)” IEEE Trans. On Power System, vol. 26, No.1,Feb. 2011.

[15] N.G. Hingorani and L. Gyugyi, Understanding FACTS, IEEE Press, 2000

[16] John J. Paserba, Nicholas W. Miller, Einar V. Larsen and Richard J. Piwko, “A Thyristor Controlled series compensation model for power system stability analysis”, IEEE Transactions on Power Delivery, Vol. 10, No. 3, July 1995.

[17] E.V.Larsen, J.J.Sanchez-Gasca and J.H.Chow, “Concepts for design of FACTS controllers to damp power swings,” IEEE Transactions on Power Systems, Vol.10, No.2, May 1995, pp.948-955

[18] N.Kumar, S.Kumar, V.Jain, "Damping subsynchronous oscillations in power system using shunt and series connected FACTS controllers," International Conference on Power, Control and Embedded Systems (ICPCES), 2010, vol., no., pp.1-5, Nov. 29 2010-Dec. 1 2010

[19] R.M. Mathur and R.K. Varma, Thyristor-Based FACTS Controllers for Electrical Transmission Systems, New York: IEEE Press and Wiley Interscience, 2002.

[20] N.G.Hingorani et al, "Prototype NGH Subsynchronous resonance damping scheme – part 1 – field installation and operating experience," IEEE Trans. Vol. PWRS-2, No.4, 1987, pp.1034-1039.

[21] L.Wang and Y. Y. Hsu, "Damping of subsynchronous resonance using excitation controllers and static VAR compensations: A comparative study," IEEE Trans. Energy Convers., vol. 3, no. 1, pp. 6–13, Mar. 1988.

[22] Y.Y.Hsu and C.J.Wu, "Design of PID Static VAR Controller for the damping of Subsynchronous Oscillations," IEEE Transactions on Energy Conversion, Vol.3, No.2, June 1988, pp.210-216

[23] S.A.Kharpade and V.Krishna, "Simulation of Unified Static VAR Compensator and Power system stabilizer for arresting subsynchronous resonance,", IEEE Trans., Power Industry Computer Applications, May 1997, pp.302-308 (Paper No.-PE-183 PWRS-16-09-1997)

[24] K. R. Padiyar and N. Prabhu, "Design and performance evaluation of subsynchronous damping controller with STATCOM," IEEE Transactions on Power Delivery, vol. 21, no. 3, pp. 1398–1405, 2006.

[25] Borre, A.C.; Ortiz, A.; Watanabe, E.H.; Sulkowski, W., "Synchronous Generator Power Oscillations Damped by Using TCSC or SSSC Working as a Variable Reactance", International Conference on Electrical Machines and Systems (ICEMS), 2011

[26] R. K. Varma, S. Auddy, and Y. Semsedini, "Mitigation of subsynchronous resonance in a series-compensated wind farm using FACTS controllers," IEEE Trans. Power Del., vol. 23, no. 3, pp. 1645–1654, Jul. 2008.

[27] H.A. Othman, L. Angquist, "Analytical modeling of thyristor-controlled series capacitors for SSR studies," Power Systems, IEEE Transactions on , vol.11, no.1, pp.119-127, Feb 1996

[28] B.K. Perkins, M.R. Iravani, "Dynamic modeling of a TCSC with application to SSR analysis," Power Systems, IEEE Transactions on Power Systems, vol.12, no.4, pp.1619-1625, Nov 1997

[29] Lennart Ängquist, Gunnar Ingeström, and Hans-Åke Jönsson, "Dynamical Performance of TCSC Schemes", CIGRÉ 1996: 14-302.

[30] Luiz A. S. Pilotto, André Bianco, Willis F. Long, and Abdel-Aty Edris,“Impact of TCSC control methodologies on subsynchronous oscillations,” IEEE Trans. Power Delivery ,vol 18, pp.243-252, Jan. 2003

[31] R.Rajaraman, I.Dobson, R.Lasseter and Y.Shern, “Computing the damping of subsynchronous oscillations due to a thyristor controlled series capacitor,” IEEE Transactions on Power Delivery, Vol.11, April 1996, pp.1120-1127

[32] N. Kakimoto, A.Phongphanphanee, "Subsynchronous resonance damping control of thyristor-controlled series capacitor," Power Delivery, IEEE Transactions on , vol.18, no.3, pp. 1051-1059, July 2003

[33] Fan Zhang and Zheng Xu, "SSR damping study on a generator connected to TCSC," Power Systems Conference and Exposition, 2004. IEEE PES , pp. 673-678 vol.2, 10-13 Oct. 2004

[34] Xiang Zheng, Zheng Xu and Jing Zhang “A Supplementary Damping Controller of TCSC for Mitigating SSR”, Power & Energy Society General Meeting, 2009. PES '09. IEEE, 2009, pp. 1-5.

[35] S.V. Jayaram Kumar, Arindam Ghosh, Sachchidanand, “Damping of subsynchronous resonance oscillations with TCSC and PSS and their control interaction”, Electric Power Systems Research, 54(2000), pp.29-36.

[36] N.Christi, R.Hedin, R.Johnson, P.Krause, “Power system studies and modelling for the Kayenta 230 kV substation advanced series compensation”, International Conference on AC and DC Power Transmission, 1991

[37] R.J.Piwko, C.A.Wegner, S.J.Kinney, J.D. Eden, "Subsynchronous resonance performance tests of the Slatt thyristor-controlled series capacitor," Power Delivery, IEEE Transactions on , vol.11, no.2, pp.1112-1119, Apr 1996

[38] D. Holmberg, M. Danielsson, P. Halvarsson, L. Ängquist, "The Stöde Thyristor-Controlled Series Capacitor", in CIGRÉ Session, Paper14-105, Paris, 1998.

[39] C. Gama, L. Ängquist, G. Ingeström, and M. Noroozian, "Commissioning and Operative Experience of TCSC for Damping Power Oscillation in the Brazilian North -South Interconnection", in Proc. CIGRÉ Session, No. 38, Paper 14-104, Paris, 2000.

[40] Chee Mun Ong, Dynamic Simulations of Electrical Machinery, Prentice-Hall PTR, 1998

APPENDIX A

IEEE First Benchmark Model

A.1 System data

The system is based on the Navajo project, and thus the base MVA is taken as 892.4 MVA while the base voltage is taken as 500 kv for the system parameters.

The parameters of the line (R_L, X_L), Transformer (X_T) and additional reactance between buses (X_{sys}) is tabulated below.

Parameter	**Positive Sequence value (pu)**	**Zero Sequence Value (pu)**
R_L	0.02	0.50
X_T	0.14	0.14
X_L	0.50	1.56
X_{sys}	0.06	0.06

The subtransient generator reactance is 0.1675 pu, while the capacitive compensation is variable.

A.2 Machine Parameters

The synchronous machine parameters are taken on a base of 892.4 MVA and 26 kv

Reactance	pu Value
x_d	1.790
x_d'	0.169
x_d''	0.135
x_q	1.710
x_q'	0.228
x_q''	0.200

Time Constant	Value (seconds)
T_{do}'	4.300
T_{do}''	0.032
T_{qo}'	0.850
T_{qo}''	0.050

A.3 Mechanical Parameters

The shaft inertia and spring constants of the system are given as follows:

Mass	**Shaft**	**Inertia H** (seconds)	**Spring constant**	
			K (pu)	**pu Torque/radian**
EXC		0.0342165		
	GEN-EXC		7277	2.822
GEN		0.868495		
	LPB-GEN		13168	70.858
LPB		0.884215		
	LPA-LPB		19618	52.038
LPA		0.858670		
	IP-LPA		26713	34.929
IP		0.155589		
	HP-IP		1064	19.303
HP		0.092897		

APPENDIX B

Park's transformation

The Park's transformation is used regularly to effect three phase to two phase transformation in synchronous machine studies. The transformation is of the form,

$$[i_{dq0}(\theta_d)] = \frac{2}{3}\begin{bmatrix} \cos\theta_d & \cos(\theta_d - \frac{2\pi}{3}) & \cos(\theta_d + \frac{2\pi}{3}) \\ -\sin\theta_d & -\sin(\theta_d - \frac{2\pi}{3}) & -\sin(\theta_d - \frac{2\pi}{3}) \\ \frac{1}{2} & \frac{1}{2} & \frac{1}{2} \end{bmatrix}[i_{abc}]$$

The inverse transformation is given by,

$$[i_{abc}] = \begin{bmatrix} \cos\theta_d & -\sin\theta_d & 1 \\ \cos(\theta_d - \frac{2\pi}{3}) & -\sin(\theta_d - \frac{2\pi}{3}) & 1 \\ \cos(\theta_d + \frac{2\pi}{3}) & -\sin(\theta_d - \frac{2\pi}{3}) & 1 \end{bmatrix}[i_{dq0}(\theta_d)]$$

Similarly, for the q component, it can be considered as either leading or lagging the d-axis component, and the transformation is correspondingly given for them.